JBC Papers in Press. Published on June 6, 2016 as Manuscript M116.718510
The latest version is at http://www.jbc.org/cgi/doi/10.1074/jbc.M116.718510

Mechanism for remodeling of the acyl chain composition of cardiolipin catalyzed by *Saccharomyces cerevisiae* tafazzin

Masato Abe, Yui Hasegawa, Masahide Oku, Yoshiki Sawada, Eriko Tanaka, Yasuyoshi Sakai, and Hideto Miyoshi

From the Division of Applied Life Sciences, Graduate School of Agriculture, Kyoto University, Sakyo-ku, Kyoto 606-8502, Japan.

Running title: Remodeling of the acyl chain composition of cardiolipin

To whom correspondence should be addressed: Hideto Miyoshi, Division of Applied Life Sciences, Graduate School of Agriculture, Kyoto University, Sakyo-ku, Kyoto 606-8502, Japan. E-mail, miyoshi@kais.kyoto-u.ac.jp. Tel: +81-75-753-6119

Keywords: tafazzin, cardiolipin, remodeling, phospholipid, lysophospholipid, acyltransferase, mitochondria

ABSTRACT

Remodeling of the acyl chains of cardiolipin (CL) is responsible for final molecular composition of mature CL after *de novo* CL synthesis in mitochondria. Yeast *Saccharomyces cerevisiae* undergoes tafazzin-mediated CL remodeling, in which tafazzin serves as a transacylase from phospholipids to monolyso-CL (MLCL). In light of the diversity of the acyl compositions of mature CL between different organisms, the mechanism underlying tafazzin-mediated transacylation remains to be elucidated. We investigated the mechanism responsible for transacylation using purified *S. cerevisiae* tafazzin with liposomes composed of various sets of acyl donors and acceptors. The results revealed that tafazzin efficiently catalyzes transacylation in liposomal membranes with highly ordered lipid bilayer structure. Tafazzin elicited unique acyl chain specificity against phosphatidylcholine (PC): linoleoyl (18:2) > oleoyl (18:1) = palmitoleoyl (16:1) >> palmitoyl (16:0). In these reactions, tafazzin selectively removed the *sn*-2 acyl chain of PC and transferred

it into the *sn*-1 and *sn*-2 positions of MLCL isomers at equivalent rates. We demonstrated for the first time that MLCL and dilyso-CL (DLCL) have inherent abilities to function as an acyl donor to monolyso-PC and acyl acceptor from PC, respectively. Furthermore, a Barth syndrome-associated tafazzin mutant (H77Q) was shown to completely lack the catalytic activity in our assay. It is difficult to reconcile the present results with the so-called thermodynamic remodeling hypothesis, which premises that tafazzin reacylates MLCL by unsaturated acyl chains only in disordered non-bilayer lipid domain. The acyl specificity of tafazzin may be one of the factors that determine the acyl composition of mature CL in *S. cerevisiae* mitochondria.

INTRODUCTION

Cardiolipin (CL), bearing two phosphate heard groups and four acyl chains, is a major phospholipid in the inner mitochondrial membrane (*1*, *2*). CL is critical for optimal mitochondrial functions, including oxidative phosphorylation, transport of substrates, formation of cristae morphology, and apoptosis (*3*-*5*). The biosynthesis of CL, which occurs in mitochondria, has been characterized in yeast *Saccharomyces cerevisiae* in detail. Phosphatidylglycerolphosphate synthase (Pgs1) catalyzes the first step of CL synthesis by converting cytidine 5'-diphosphate-diacylglycerol (CDP-DAG) and glycerol-3-phosphate (G3P) to produce phosphatidylglycerolphosphate (PGP) (*6*). PGP is dephosphorylated to phosphatidylglycerol (PG) by the PGP phosphatase Gep4 (*7*) (PTPMT1 in mammals, refs. *8* and *9*). CL synthase (Crd1) catalyzes the final step of CL synthesis by condensing PG and another molecule of CDP-DAG to produce CL, which is immature CL with primarily saturated acyl chains of various lengths (*10*, *11*).

Following the *de novo* synthesis of CL on the matrix side of the inner mitochondrial membrane (*12)*, acyl chain remodeling is responsible for the final molecular composition of mature CL, which is typically defined by the symmetric incorporation of unsaturated fatty acyl chains (*13*). In this process, CL is deacylated to monolyso-CL (MLCL) by CL-specific lipase Cld1 (*14*). The reacylation of MLCL is accomplished by three distinct proteins in higher eukaryotes; tafazzin, monolysocardiolipin acyltransferase 1 (MLCLAT1), and acyl-CoA:lysocardiolipin acyltransferase-1 (ALCAT1), whereas yeast only undergoes tafazzin-mediated reacylation. Although MLCLAT1 and ALCAT1 utilize acyl-CoA as the acyl chain donor for the reacylation of MLCL (*15*, *16*), tafazzin is a transacylase that takes an acyl chain from another phospholipid, preferentially phosphatidylcholine (PC) or phosphatidylethanolamine (PE), and adds

it to MLCL (*17*). Mutations in tafazzin cause Barth syndrome, resulting in cardio- and skeletal myopathy and respiratory chain defects (*18*, *19*). In Barth syndrome patients and models of Barth syndrome, the CL/MLCL ratio is decreased and the remaining CL contains an altered acyl chain composition (e.g. low content of unsaturated acyl chains) (*20*-*23*).

Since tafazzin exhibits little acyl chain specificity among potential phospholipid substrates (namely, this enzyme randomly reacts with virtually all phospholipid and MLCL species) (*13*, *17*), the acyl chain compositions of all CLs may become identical if they are exposed to tafazzin for a sufficient period of time; however, this is not the case (*24*). Therefore, a critical question is how tafazzin causes specific patterns of acyl chains in mature CL; for example, tetralinoleoyl (18:2)-CL is a major CL in mammalian heart, and oleic (18:1) and palmitoleic (16:1) acids are major acyl chains in yeast mitochondrial CL (*25*).

Schlame and colleagues investigated whether purified *Drosophila melanogaster* tafazzin (*17*) can replicate the remodeling of CL *in vitro*. They demonstrated that efficient transacylation from phospholipids to MLCL *only* occurs in non-bilayer lipid aggregates (e.g. the inverted hexagonal lipid phase), and not in ordered lipid bilayer membrane like liposomes (*26*). Acyl chain specificity was also shown to be highly sensitive to the lipid structural order; namely, a remarkable preference for linoleoyl (18:2) over oleoyl (18:1) groups was only observed in non-bilayer lipid membranes (*26*). Based on these findings, they proposed the so-called thermodynamic remodeling hypothesis to explain acyl specificity in the tafazzin-mediated remodeling of CL (*26*); tafazzin functions at non-bilayer-type relaxed lipid domains, which occur in curved membrane domains, because of the preferential mixing of phospholipids and MLCL species, and its acyl specificity is driven by the packing properties of these domains. In other words, multiple transacylations will change the acyl chain composition of CL until their free energy is minimal, at which point the chain composition is optimal for specifically curved membrane domains (*27*). CL, which has a relatively small volume of polar head group and unsaturated acyl chains (such as linoleic acid), has a shape asymmetry that preferentially leads to its accumulation in negatively curved lipid monolayer (*28*).

Nevertheless, in light of the diversity of acyl chain compositions of CL in different organisms or even in tissues within the same organism, it currently remains unclear whether the thermodynamic remodeling hypothesis accounts for all details of tafazzin-mediated CL remodeling. For example, Schlame et al.

reported that only a portion (<1%) of endogenous mitochondrial phospholipids participates in transacylation (PLs + [^{14}C]lyso-PC (LPC) → LPLs + [^{14}C]PC) (*26*), suggesting that the action of tafazzin is highly limited to specific mitochondrial domains. However, this finding is difficult to reconcile with the fact that mammalian heart mitochondria contain an extremely high content of the uniform acyl chain composition, tetralinoleoyl-CL (~80% of all CL, ref. *29*); which indicates that a large extent of the remodeling of CL takes place in this organ. Although mitochondria contain curve-shaped membrane domains (the cristae), it has not yet been established whether there are substantial domains that are sufficiently curved to be categorized as non-bilayered membrane domain (*30*). Furthermore, hexagonal and micellar phases have both shown to facilitate tafazzin-mediated transacylation (*26*), which is unexpected because the two lipid states are characterized by opposite curvatures of the lipid-water interface. The shape of CL makes it favorable for being positioned at negatively curved membrane regions (*28*), as mentioned above. Thus, it is still debatable whether the thermodynamic remodeling hypothesis is a general feature of tafazzin-mediated transacylation. A critical point to be verified is whether transacylation accompanying the remarkable acyl specificity [linoleoyl (18:2) >> oleoyl (18:1)] from PC to MLCL *only* occurs in non-bilayer lipid aggregates, and not in ordered lipid bilayer membranes.

We herein investigated the mechanism underlying tafazzin-mediated transacylation using purified *S. cerevisiae* tafazzin with a liposomal system composed of various pairs of PC (acyl donor) and MLCL (acyl acceptor) species (Figure 1). Since all CL species used in this study were synthesized according to the procedures developed in our laboratory (*31-33*), we were able to arbitrarily fix their acyl chain compositions. The present study clearly demonstrated that *S. cerevisiae* tafazzin catalyzes efficient transacylation among phospholipid substrates even with the liposomal system, highly ordered lipid bilayer environment. Tafazzin elicited unique acyl chain specificity against PC: linoleoyl (18:2) > oleoyl (18:1) = palmitoleoyl (16:1) >> palmitoyl (16:0). On the basis of these results, we conclude that the thermodynamic remodeling hypothesis is not necessarily a general scenario to describe the mechanism underlying tafazzin-mediated CL-remodeling. The substrate specificity of tafazzin may be one of the factors that determine the acyl composition of mature CL.

RESULTS

Effects of the GST tag and Ca^{2+} on the Catalytic Activity of Tafazzin

We investigated transacylation from PC to MLCL catalyzed by isolated *S. cerevisiae* GST-tagged tafazzin with liposomes, highly ordered lipid bilayer environment. The PC:MLCL molar ratio was fixed at 9:1 throughout this study in order to maintain ordered lipid bilayer structure (*34*, *35*). We preliminarily examined the effects of two factors (the GST tag and Ca^{2+}) on the catalytic activity of tafazzin to optimize the reaction conditions.

To determine the effect of the GST tag on the catalytic activity of tafazzin, we compared activities between GST-tagged and tag-free enzymes in the reaction [PC(18:1-18:1) + *sn*-2'-MLCL(18:1-18:1/18:1-OH) → LPC + CL(18:1-18:1/18:1-18:1)]. The results obtained showed that the GST tag did not affect enzyme activity (Figure 2, column *b*). Therefore, we used GST-tagged tafazzin throughout this study because of the less laborious purification process. In this and following experiments, transacylation did not occur in the absence of tafazzin (Data not shown); therefore, mere chemical reaction was not responsible for the transacylation observed.

Schlame et al. previously used a high concentration of Ca^{2+} (20 mM) to prepare inverted hexagonal lipid phase from lipid mixture dispersion (*26*). Since the possibility that a high concentration of Ca^{2+} affects the catalytic activity of tafazzin cannot be excluded, we investigated the effect of Ca^{2+} (1 and 20 mM) on enzyme activity in the reaction [PC(18:1-18:1) + *sn*-2'-MLCL(18:1-18:1/18:1-OH) → LPC + CL(18:1-18:1/18:1-18:1)]. Enzyme activity determined in the presence of 1 mM Ca^{2+} was almost identical to that determined in the absence of Ca^{2+}, but was reduced by ~30% in the presence of 20 mM Ca^{2+} (Figure 2, columns *c* and *d*). Since the presence of high concentrations of Ca^{2+} was unfavorable for tafazzin-mediated transacylation under our experimental conditions, we omitted Ca^{2+} from the reaction mixture in this study.

The sn-2 Acyl Chain of PC is Selectively Transferred to Monolyso-CL

In tafazzin-mediated acyl transfer from PC to MLCL, the acyl chain of PC (*sn*-1, *sn*-2, or both positions) that is deacylated has not yet been identified. This hitherto unresolved issue is important to obtain a more comprehensive understanding mechanism underlying the tafazzin-mediated transacylation. To investigate this issue, *sn*-1-LPC and *sn*-2-LPC are needed as the standard samples. It is the general nature of lyso-phospholipids that the acyl group in the *sn*-2 position tends to migrate

to the *sn*-1 position if the *sn*-1 position is deacylated (i.e. free glycerol OH) (*31, 36, 37*). Therefore, we carefully synthesized *sn*-1-LPC(OH-18:1) and *sn*-2-LPC(18:1-OH) separately (Figure 1). Judging from their ^{1}H NMR spectra, a content of *sn*-2-LPC(18:1-OH), which was formed by automigration during the synthetic and/or purification processes, in *sn*-1-LPC(OH-18:1) sample was ~5%.

We established HPLC (detected by ELSD, Figure 3A) and ESI-LC/MS [detected by a selected ion (*m*/*z* 522.4) monitoring mode, Figure 3B] analytical conditions to determine *sn*-1-LPC(OH-18:1) and *sn*-2-LPC(18:1-OH). Considering a content of *sn*-2-LPC(18:1-OH) (~5%) in *sn*-1-LPC(OH-18:1) sample, the results shown in Figure 3A(i) and 3B(i) indicated that the extent of automigration from *sn*-1-LPC(OH-18:1) to *sn*-2-LPC(18:1-OH) is negligibly small under the analytical conditions. The analytical results of *sn*-2-LPC(18:1-OH) were shown in Figure 3A(ii) and 3B(ii).

We then analyzed LPC produced in the reaction [PC(18:1-18:1) + *sn*-2'-MLCL(18:1-18:1/18:1-OH) → LPC + CL(18:1-18:1/18:1-18:1)], which was almost complete within ~1 h. The averaged ratios of *sn*-2-LPC(18:1-OH):*sn*-1-LPC(OH-18:1) determined by HPLC and ESI-LC/MS analyses after a 40 min reaction were 98:2 [Figure 3A(iii)] and 93:7 [Figure 3B(iii)], respectively, indicating that the deacylation of PC occurred predominantly at the *sn*-2 position. We also confirmed this regiospecificity in the deacylation of PC in the following transacylation experiments.

Tafazzin-Mediated Transfer of Oleoyl (18:1) or Linoleoyl (18:2) Group from PC to sn-2-Monolyso-CL

In an attempt to elucidate the effects of acyl chain compositions on tafazzin-mediated transacylation, we used two different PC and *sn*-2-MLCL species as acyl donors and acceptors, respectively: PC(18:1-18:1) and PC(18:2-18:2), and *sn*-2'-MLCL(18:1-18:1/18:1-OH) and *sn*-2'-MLCL(18:2-18:2/18:2-OH). Previous studies from different laboratories (*17*, *23*, *24*, *26*, *38*) evaluated the catalytic activity of tafazzin by determining the amounts of lipids produced after a certain reaction period by means of counting the radioactivity of ^{14}C-incorporated products or a quantitative MALDI-TOF MS analysis. However, since any kinetic parameter of the catalytic reaction cannot be evaluated by such single-point measurements, we herein followed the time-course of the formation of the product of interest.

Efficient acyl transfer from PC to *sn*-2-MLCL was observed in all donor-acceptor

pairs even in liposomes, as shown in Figure 4A taking the reactions [PC(18:2-18:2) + *sn*-2'-MLCL(18:1-18:1/18:1-OH) → *sn*-2-LPC(18:2-OH) + CL(18:1-18:2/18:1-18:1)] and [PC(18:1-18:1) + *sn*-2'-MLCL(18:1-18:1/18:1-OH) → *sn-2*-LPC(18:1-OH) + CL(18:1-18:1/18:1-18:1)] as examples. The pseudo-first-order rate constants (*k*), estimated by a modified Guggenheim plot (Figure 4B, *ref. 39*), were summarized in Table 1. Our results demonstrated that PC(18:2-18:2) is slightly superior to PC(18:1-18:1) as an acyl donor to *sn*-2-MLCL; the rate constants of the former were ~1.5-fold greater than those of the latter. It is important to note that the remarkable preference for linoleoyl (18:2) over oleoyl (18:1) groups, as reported for *D. melanogaster* tafazzin (*26*), was not observed for yeast tafazzin. The acyl chain composition of *sn*-2-MLCL did not significantly affect its ability as an acyl acceptor [*sn*-2'-MLCL(18:1-18:1/18:1-OH) vs. *sn*-2'-MLCL(18:2-18:2/18:2-OH)] (Table 1).

To know whether CL, which contains two or more acyl groups transferred from PC, is produced if the incubation of MLCL with PC is prolonged, we prolonged the incubation over the period of ~3 h using liposomes composed of PC(18:2-18:2) and *sn*-2'-MLCL(18:1-18:1/18:1-OH) at a 9:1 ratio. A chromatographic peak(s) corresponding to a new product(s), besides CL(18:1-18:1/18:1-18:2), was not detected by HPLC analysis. To further address this point, we also examined whether transacylation occur between PC(18:2-18:2) and CL(18:1-18:1/18:1-18:2) using liposome composed of PC(18:2-18:2) and CL(18:1-18:1/18:1-18:2) at a 9:1 ratio; however, no new chromatographic peak of product was detected.

Furthermore, to investigate effects of membrane components on the catalytic activity of tafazzin, we also examined the reaction using liposomes composed of PC(18:2-18:2) and *sn*-2-MLCL(18:1-18:1/18:1-OH) at a 8:2 molar ratio. The mean diameter of liposomes made up of the 8:2 mixture was identical to that of liposomes of the 9:1 mixture (Data not shown). Although the apparent reaction rate observed with the 8:2 mixture was considerably faster (by ~1.3-fold) than that with the 9:1 mixture, the rate constants were almost identical between the two reactions (0.10 ± 0.02 min^{-1} for 8:2 vs. 0.098 ± 0.008 min^{-1} for 9:1).

Tafazzin-Mediated Transfer of Palmitoyl (16:0) or Palmitoleoyl (16:1) Group from PC to Monolyso-CL

The content of palmitoyl (16:0) group in PC and PE species is as high as that of palmitoleoyl (16:1) group in *S. cerevisiae* mitochondria (*14*),

whereas palmitoleoyl group, but not palmitoyl group, is a major acyl component of mature CL (*25*, *40*). In an attempt to obtain more information, we determined whether tafazzin transacylates palmitoyl group between PC(16:0-16:0) and *sn*-2'-MLCL(18:1-18:1/18:1-OH) to produce CL(18:1-18:1/18:1-16:0) using liposomes (PC:MLCL, 9:1 molar ratio). Surprisingly, tafazzin did not virtually catalyze the reaction; the amount of CL(18:1-18:1/18:1-16:0) produced after a 40 min reaction was less than 0.3 nmol. The rate constant was not estimated because of very poor activity (Table 1). We also examined transacylation between PC(16:0-16:0) and *sn*-1'-MLCL(18:1-18:1/OH-18:1), and found that tafazzin, again, did not virtually catalyze the reaction to produce CL(18:1-18:1/16:0-18:1).

In contrast, tafazzin efficiently transacylated palmitoleoyl group from PC(16:1-16:1) to *sn*-2'-MLCL(18:1-18:1/18:1-OH) and *sn*-1'-MLCL(18:1-18:1/OH-18:1); the rate constants were comparable to those observed for PC(18:1-18:1) (Table 1). Thus, a remarkable acyl specificity in tafazzin-mediated transacylation was observed between PC(16:0-16:0) and PC(16:1-16:1). This result is important when considering the mechanism underlying CL remodeling in *S. cerevisiae* mitochondria, as discussed later.

There may be two possibilities as the cause of the poor transacylation activity for PC(16:0-16:0); one is that tafazzin cannot remove palmitoyl group from PC and the other is that tafazzin has this ability, but cannot transfer it to MLCL. To verify these two possibilities, we determined the amount of PC(16:0-16:0) remaining in the reaction mixture after the 40 min reaction by HPLC analysis, and found that the residual amount is almost identical to the initial amount (a total of ~45 nmol). This result strongly suggests that tafazzin does not have the ability to remove palmitoyl group from PC.

The above results raised another question; can tafazzin remove palmitoyl group from CL and attach it to LPC? Since this question would be important to consider the role of phospholipase in CL remodeling, we investigated acyl transfer using liposome composed of CL(16:0-16:0/16:0-16:0), *sn*-2-LPC(18:1-OH), and PC(18:1-18:1) at a 1:1:8 molar ratio. A large portion of PC(18:1-18:1) was used to prepare unilamellar vesicles. An anticipated product PC(18:1-16:0) was synthesized as a standard compound for HPLC analysis. As a result, production of PC(18:1-16:0) was not detected within ~1.5 h incubation, indicating that tafazzin dose not transfer palmitoyl group from CL to LPC.

Regiospecificity of Tafazzin-Mediated Transacylation from PC to Monolyso-CL Isomers

All four acyl chains of CL participate in the tafazzin-mediated remodeling process, which requires a mechanism that does not discriminate between the *sn*-1- and *sn*-2-glycerol positions. Using two MLCL isomers (*sn*-1-MLCL and *sn*-2-MLCL), which lack one of the four acyl groups at the *sn*-1 or *sn*-2 position, Malhotra et al. demonstrated that tafazzin transfers an acyl group into *sn*-1 and *sn*-2 positions at almost equally efficient rates (*24*). Nevertheless, because the features of tafazzin-mediated transacylation were significantly different between previous studies (*24*, *26*) and our work, as described so far, we reinvestigated the regiospecificity of acyl transfer from PC to MLCL isomers by comparing the reaction rates of *sn*-1'-MLCL(18:1-18:1/OH-18:1) and *sn*-1'-MLCL(18:2-18:2/OH-18:2) with those of *sn*-2'-MLCL(18:1-18:1/18:1-OH) and *sn*-2'-MLCL(18:2-18:2/18:2-OH), respectively.

We carefully synthesized *sn*-1-MLCL species and handed them in subsequent experiments to avoid automigration of the acyl group in the *sn*-2 position, as mentioned above. *sn*-1 and *sn*-2-MLCL isomers were determined accurately based on their ^{1}H NMR spectra (Figures 5A and 5B); *sn*-1-MLCL, but not *sn*-2-MLCL, yielded a specific resonance signal at ~5.0 ppm, which is characteristic of the $POCH_2$–C**H**(OR)–CH_2OH proton [H(8) in Figure 5A]. The ^{1}H NMR spectra of our *sn*-1-MLCL samples indicated that the contents of *sn*-2 isomers are less than 5%, as shown in Figure 5A taking *sn*-1'-MLCL(18:1-18:1/OH-18:1) as an example.

We established a HPLC analytical method that enables discrimination between *sn*-1-MLCL and *sn*-2-MLCL. Figure 5C shows an example of the HPLC charts observed for (i) *sn*-1'-MLCL(18:1-18:1/OH-18:1) alone, (ii) *sn*-2'-MLCL(18:1-18:1/18:1-OH) alone, and (iii) a mixture of them, which indicated that the extent of automigration is negligibly small under the HPLC analytical conditions. By the HPLC analysis of MLCL isomers recovered from the assay mixtures with or without tafazzin, we also confirmed that no significant migration occurs during the assay process or the preparation of liposomes (Data not shown). On the other hand, judging from ^{1}H NMR spectra reported in ref. *24*, a small fraction of *sn*-2-MLCL (~20%) was included in the previous *sn*-1-MLCL sample that was prepared by treating commercially available CL with *R. arrhizus* lipase, which removes an acyl chain preferentially from the *sn*-1 position. It is unclear whether the authors checked the automigration in subsequent experiments.

As summarized in Table 1, we corroborated that tafazzin is able to efficiently transfer an acyl group into the *sn*-1 and *sn*-2 positions of MLCL isomers; there was no preference for the glycerol positions. The acyl chain compositions of acyl donors and acceptors did not significantly affect this feature. It is noteworthy that the slightly greater preference for PC(18:2-18:2) than PC(18:1-18:1) as an acyl donor was again observed with *sn*-1-MLCL, as noted with *sn*-2-MLCL. The lack of regiospecificity in tafazzin-mediated transacylation is a prerequisite for uniformity and/or symmetry in the acyl distribution of CL (*24*).

Monolyso-CL Functions as an Acyl Donor to lyso-PC

Using commercially available MLCL and DLCL, Malhotra et al. demonstrated that the role of MLCL in tafazzin-mediated transacylation is limited to that of an acyl acceptor from phospholipids to produce CL, and DLCL does not function as an acyl acceptor (*24*). Based on this information, the authors designed acyl donor-acceptor pairs for transacylation experiments in their subsequent study (*26*). However, if MLCL serves as an acyl donor, the complexity of transacylation patterns may markedly increase. Therefore, it is important to clarify whether MLCL serves as an acyl donor for other lyso-phospholipids.

We examined this issue using a MLCL-LPC mixture at a 1:9 molar ratio [*sn*-2'-MLCL(18:1-18:1/18:1-OH) + *sn*-2-LPC(18:1-OH) → DLCL + PC(18:1-18:1)]. Dynamic light scattering measurement revealed that this lipid mixture failed to form liposomes, but may form micelle-like morphology with an averaged diameter of ~20 nm, which is drastically smaller than that of liposomes prepared from other acyl donor-acceptor pairs (an averaged diameter of ~110 nm). This may be due to the lack of PC as a major component when preparing liposomes. We note that PC was not used in this reaction because substantial transacylation occurs from PC to LPC and MLCL.

As shown in Figure 6, the amount of *sn*-2-MLCL in the reaction medium gradually decreased, whereas the reaction was almost complete after ~5 h with ~20% consumption of initial *sn*-2-MLCL. We detected the production of PC(18:1-18:1), the amount of which corresponds to that of consumed *sn*-2-MLCL. The unique lipid phase of this lipid mixture may be responsible for the incomplete reaction. We were able to identify the acyl composition of the DLCL produced as *sn*-2/*sn*-2'-DLCL(18:1-OH/18:1-OH) by a HPLC analysis using synthetic DLCL isomers as the standard samples, which have two oleoyl groups at the *sn*-1–*sn*-1', *sn*-1–*sn*-2', or

sn-2–*sn*-2' position (Figure 1), and their averaged retention times were 13.8, 14.7, and 15.5 min, respectively. This result indicates that an oleoyl group in the *sn*-2 position of *sn*-2-MLCL was selectively transferred to *sn*-2-LPC to produce PC. Thus, our results clearly reveal that MLCL has an inherent ability as an acyl donor.

In this reaction, we cannot exclude the possibility that *sn*-2-MLCL was once transformed to CL(18:1-18:1/18:1-18:1) by accepting an oleoyl chain from *sn*-2-LPC, and then CL afforded an oleoyl chain to the remaining *sn*-2-LPC(18:1-OH) to produce PC(18:1-18:1). Although the likelihood of this is very low because, if so, *sn*-2-LPC further loses the remaining acyl group, we attempted to detect the possible intermediate CL during the reaction course. However, we were unable to detect any CL, indicating that *sn*-2-MLCL functions as a direct acyl donor to *sn*-2-LPC. This result simultaneously indicates that no transacylation occurs between two *sn*-2-MLCL molecules to produce CL and *sn*-2/*sn*-2'-DLCL.

Dilyso-CL Functions as an Acyl Acceptor from PC

The above result that MLCL serves as an acyl donor to provide DLCL prompted us to investigate whether DLCL serves as an acyl acceptor from another CL (or MLCL) as well as PC in the tafazzin-mediated reaction. The significant accumulation of DLCL (along with MLCL) was previously reported for tafazzin knock-down mouse model of Barth syndrome (*41*). Therefore, we examined acyl transfer from PC to DLCL at a molar ratio of 9:1 [PC(18:1-18:1) + *sn*-2/*sn*-2'-DLCL(18:1-OH/18:1-OH) → *sn*-2-LPC(18:1-OH) + *sn*-2'-MLCL(18:1-18:1/18:1-OH)].

As shown in Figure 7A, *sn*-2/*sn*-2'-DLCL was efficiently converted to *sn*-2-MLCL (*open circles*). The rate constant for this reaction (0.072 ± 0.005 min^{-1}) was similar to that determined for transacylation from PC(18:1-18:1) to *sn*-2'-MLCL(18:1-18:1/18:1-OH) (Table 1). Since we detected the formation of a small fraction of CL(18:1-18:1/18:1-18:1) (*closed circles*) during the first 20 min, we continued to monitor the formation of CL. The amount of CL gradually increased with a slight decrease in the total amount of *sn*-2-MLCL (Figure 7B). Taking the inherent transacylation ability of tafazzin into consideration, it is feasible that, once formed, *sn*-2-MLCL was further transformed to CL by accepting an acyl chain from PC. However, this (second) transacylation reaction was significantly slower than that observed for the direct production of CL from a mixture of *sn*-2-MLCL and PC (e.g.

Figure 4A). This may be because the initial concentration of *sn*-2-MLCL in the former was significantly lower than that in the latter. The total amount of *sn*-2-MLCL and CL produced after ~400 min was almost equivalent to the initial amount of *sn*-2/*sn*-2'-DLCL (5.0 nmol), indicating that almost all *sn*-2/*sn*-2'-DLCL was transformed to these CL species during the reaction. In contrast to previous findings (*24*), our results clearly demonstrated that MLCL and DLCL function as an acyl donor to LPC and acyl acceptor from PC, respectively, in tafazzin-mediated transacylation.

Transacylation Activity of the H77Q Mutant

Claypool and colleagues established Barth syndrome-associated tafazzin mutants in *S. cerevisiae* mitochondria and classified them into seven functional classes based on their biochemical and cell biological characterization (*23*, *38*). Of the seven classes, the class 4 mutations resulted in catalytic inactive tafazzin, although expression levels, localization in mitochondria, and assembly in macromolecular complexes were almost normal. H77 is located in the HX_4D motif, a conserved structural motif in acyltransferase, and the H77Q mutant is a typical example of the class 4 mutants (*23*). We prepared the H77Q mutant, and isolated and determined its transacylation activity in the reaction [PC(18:2-18:2) + *sn*-2'-MLCL(18:1-18:1/18:1-OH) → *sn*-2-LPC(18:2-OH) + CL(18:1-18:1/18:1-18:2)]. Our results showed that this mutant almost completely lacks the catalytic activity in our model membrane system (Figure 2, column *e*), as observed with the assay using *S. cerevisiae* mitochondria [phospholipids (in mitochondria) + [^{14}C]MLCL → [^{14}C]CL] (*23*). Lu et al. recently demonstrated that the human equivalent of the H77Q mutant (H69Q in human) remarkably lacks the transacylation activity (*42*), indicating conservation of the functional importance of this histidine.

DISCUSSION

Since tafazzin is considered to exhibit little acyl chain selectivity among possible phospholipid substrates (*1*, *17*), the mechanism by which it determines the acyl chain composition of mature CL has yet to be explained. The thermodynamic remodeling hypothesis (*26*) appears to ingeniously explain the marked enrichment of CL fraction of *D. melanogaster* and mammalian mitochondria with CL(18:2-18:2/18:2-18:2). This hypothesis, in principle, is based on the idea that tafazzin reacts only at non-bilayer-type lipid domains, which may occur in curved membrane zones, and the specificities of acyl chain compositions are derived from the physical properties of these domains (i.e. lipid packing). In other words,

highly curved membranes promote the catalytic reaction of tafazzin with multi-unsaturated acyl chains, and tafazzin, in turn, stabilizes the membrane curvature (*26*, *27*). To verify this hypothesis, it is critical to prove that tafazzin does not function in the reacylation of MLCL by an unsaturated acyl chain in structurally ordered lipid bilayer membrane. Schlame and colleagues did not necessarily prove this issue in the strict sense because they used the dispersion of acyl donor-acceptor lipid mixtures, which were prepared by sonication for 2 min in a bath-type sonicator (*26*). On the basis of the chemical shift anisotropy of magic angle spinning ^{31}P-NMR, they regarded the lipid phase primarily as hexagonal and lamellar phases in the presence and absence of 20 mM Ca^{2+}, respectively; the former is less structural ordered than the latter. However, it may be difficult to unequivocally define the phases (or polymorphism) of lipid dispersion solely by the ^{31}P-NMR technique under their experimental conditions. Therefore, we herein investigated this issue with unilamellar liposomes, ordered lipid bilayer membranes, using purified *S. cerevisiae* tafazzin.

The results of the present study revealed that isolated tafazzin efficiently catalyzes transacylation from PC possessing unsaturated acyl chains to MLCL, even in liposomes. The acyl donors (PC) exhibited a slight, but not strong (*26*) preference for linoleoyl (18:2) over oleoyl (18:1) groups irrespective of the acyl chain compositions of the acyl acceptors (MLCL). In these reactions, tafazzin selectively removed the *sn*-2 acyl chain of PC and transferred it into the *sn*-1 and *sn*-2 positions of MLCL isomers at almost equivalent rates. It is important to note that tafazzin exhibited the remarkable acyl specificity for PC; it substantially transferred palmitoleoyl (16:1) group, but not palmitoyl (16:0) group in PC to MLCL. Moreover, we revealed for the first time that *sn*-2-MLCL and *sn*-2/*sn*-2'-DLCL have inherent abilities to function as an acyl donor to *sn*-2-LPC and an acyl acceptor from PC, respectively, in the tafazzin-mediated *in vitro* reaction. However, it currently remains unclear whether *sn*-2-MLCL and *sn*-2/*sn*-2'-DLCL actually function as an acyl donor and acceptor, respectively, in CL remodeling in mitochondria. Additionally, we corroborated that H77, located in the conserved structural motif (HX_4D) of acyltransferase, is critical for the catalytic activity. Collectively, we conclude that the thermodynamic remodeling hypothesis is not necessarily a general scenario to describe the mechanism underlying tafazzin-mediated CL remodeling, at least for *S. cerevisiae* tafazzin. On the basis of our results, we will discuss the mechanism responsible for CL remodeling later.

Some discrepancies concerning the features of tafazzin-mediated transacylation exist between earlier studies (*24*, *26*) and our work. In order to identify these discrepancies, we compared the specific activity of isolated tafazzin between both studies, taking the reaction [PC(18:2-18:2) + *sn*-2'-MLCL(18:2-18:2/18:2-OH) → LPC(18:2-OH) + CL(18:2-18:2/18:2-18:2)] as an example. Note that Schlame and colleagues used CL(18:1-18:1/18:1-18:1)–*sn*-2'-MLCL(18:2-18:2/18:2-OH)–*sn*-2-LPC(18:1-OH)–PC(18:2-18:2) mixtures with various molar ratios to investigate this reaction (see Figure 5 in ref. *26*). The averaged specific activity of our enzyme was markedly higher than the highest activity reported in their study (~20 *vs.* ~1.5 pmol CL/min/μg of tafazzin). Although we are unable to specify a critical causal factor for this difference, it may be related to differences in the origin as well as the expressed form of tafazzin; namely, *D. melanogaster* MBP (~43 kDa)-tagged tafazzin and *S. cerevisiae* GST (~27 kDa)-tagged tafazzin were used in the earlier study (*24*, *26*) and our work, respectively. We confirmed that the existence of the GST tag does not affect the catalytic activity of *S. cerevisiae* tafazzin. Based on previous findings (*17*, *24*, *26*), it is unclear whether the MBP tag affects the catalytic activity of *D. melanogaster* tafazzin. Moreover, besides differences in the origin and expressed form of tafazzin, we may not exclude possible differences in the morphological states of lipid mixtures (liposome *vs*. lipid dispersion), which are substrates of tafazzin as well as the microenvironment in which tafazzin works. It is also important to stress that our HPLC analytical method enabled the accurate quantification of the lipids produced because of diminishing sample loss by omitting the extraction step of the lipids with an organic solvent(s) (see Experimental Procedures).

The results of this study demonstrated unique acyl chain specificity in tafazzin-mediated transacylation from PC to MLCL: linoleoyl (18:2) > oleoyl (18:1) = palmitoleoyl (16:1) >> palmitoyl (16:0). Nevertheless, the mechanism underlying CL remodeling in mitochondria may not be described solely by the functions of tafazzin. Contribution of other enzymes to CL remodeling has been discussed such as Cld1 (*43*) and enzymes with lysophospholipid:acyl-CoA acyltransferase activity, MLCLAT1 (*15*) and ALCAT1 (*16*). In particular, Cld1, which is a CL-specific phospholipase and predominantly removes saturated acyl groups such as palmitoyl and stearoyl (18:0) groups (*14*), may play an important role in the initiation of CL remodeling in yeast mitochondria (*40*, *44*). The present observations that tafazzin could not efficiently

remove palmitoyl group from PC and CL support this notion. Although the content of palmitoyl group in PC and PE species (i.e. acyl donors) is as high as that of palmitoleoyl group in yeast mitochondria (*14*), palmitoleoyl and oleoyl groups are two major acyl components of mature CL (*25*, *40*). The enrichment of these acyl groups in yeast CL may be explained by the preferential removal of saturated palmitoyl and stearoyl groups from *de novo* synthesized CL by Cld1 to provide MLCL (*14*, *40*) and the subsequent tafazzin-mediated reacylation of MLCL by oleoyl and/or palmitoleoyl groups, but not palmitoyl, in PC. The enrichment of linoleoyl group in CL may not be feasible because its content in PC and PE species is originally low in yeast mitochondria (*14*). Thus, CL remodeling may require the coordinated action of phospholipase(s) and transacylase(s), such as tafazzin. Nevertheless, since tafazzin and Cld1 (both contain no transmembrane segment) are associate with the intermembrane space-facing and matrix-facing leaflets of the mitochondrial inner membrane, respectively (*4*, *45*), MLCL generated by Cld1 must be transported to the intermembrane space-facing leaflet to gain access to tafazzin, suggesting the existence of an as yet unidentified protein(s) capable of redistributing MLCL across the inner membrane. Further studies are needed to establish all of the involved players and elucidate their roles in CL remodeling in mitochondria.

Information on the physiological importance of the regulation of CL remodeling remains very limited, thereby preventing a more comprehensive molecular understanding of how this clinically relevant process promotes mitochondrial functions. Two groups recently and independently showed that defined changes in the acyl chain composition of CL do not significantly alter either the mitochondrial morphology or mitochondrial bioenergetic functions in yeast (*40*, *44*). Both groups suggested alternative physiological roles for the CL remodeling process; for example, a repair mechanism that removes and replaces acyl chains damaged by oxidative stress, thereby restoring the oxidative phosphorylation capacity of mitochondria (*40*, *44*).

EXPERIMENTAL PROCEDURES

Material

1,2-Dioleoyl-*sn*-glycero-3-phosphatidylcholine, 1,2-dilinoleoyl-*sn*-glycero-3-phosphatidylcholine, 1,2-dipalmitoyl-*sn*-glycero-3-phosphatidylcholine, and 1,2-dipalmioleoyl-*sn*-glycero-3-phosphatidylcholine were purchased from NOF Corp. (Tokyo, Japan), Santa Cruz Biotechnology (Santa Cruz, CA), Wako Pure Chemical Ltd. (Tokyo, Japan),

and Avanti Polar Lipid Inc. (Alabaster, AL) respectively. Lipase from *Mucor javanicus* and phospholipase A_2 (PLA_2) from the porcine pancreas were purchased from Sigma-Aldrich (St. Louis, MO).

Synthesis of PC and CL Analogues and Their Abbreviated Designation

The PC and CL analogues synthesized in the present study are shown in Figure 1. The synthetic procedures for these phospholipids are described in Supplemental Data. We used abbreviated designations for PC and CL analogues in order to characterize their acyl compositions with discrimination between the *sn*-1 and *sn*-2 glycerol positions. The former and latter figures in the parentheses represent the acyl group in the *sn*-1 and *sn*-2 positions, respectively; for example, PC(18:2-18:1) means PC having linoleoyl and oleoyl groups in the *sn*-1 and *sn*-2 positions, respectively, and *sn*-2'-MLCL(18:1-18:1/18:1-OH) means monolyso-CL that has three oleoyl groups in the *sn*-1, *sn*-2, and *sn*-1' positions, but lacks an acyl chain in the *sn*-2' position of one glycerol moiety.

Preparation of S. cerevisiae *Tafazzin and its H77Q Mutant*

The ORF of the *S. cerevisiae* gene encoding tafazzin (TAZ1, YPR140w) was amplified by PCR using KOD Fx Neo DNA polymerase (Toyobo, Japan), with the genome gained from the BY4741 strain used as a template DNA and the oligonucleotides (ScTaz1InfusionFw: TCGAAACGAGGAATTCATGTCTTTTAGG GATGTCCTAGAAAGA; ScTaz1InfusionRv: GAGTTTTTGTTCTAGATCATCCTTACCCT TTGGTTTACC) as primers. The amplified fragment was introduced into the pGEX6P-1 vector (GE Healthcare, Japan) linearized with *Eco* RI and *Not* I restriction enzymes (New England Biolabs, Japan), using an In-fusion HD Cloning kit (Takara Bio, Japan) to yield the pGST-Taz1 plasmid. To prepare a point-mutated derivative of the yeast tafazzin (H77Q), mutagenesis PCR was performed using PrimeStar Max DNA polymerase (Takara Bio, Japan) with pGST-Taz1 as a template and the oligonucleotides (ScTaz1H77Qfw: CCTTATGACGGTCATGAACCAAATGAGT ATGGTCGATGATCCG; ScTaz1H77QRv: CGGATCATCGACCATACTCATTTGGTTCA TGACCGTCATAAGG) as primers, which produced the pGST-Taz1H77Q plasmid.

Esherichia coli Rosetta (DE3)pLysS (Merck Millipore, Japan) strains harboring the constructed plasmids were used for the expression of yeast tafazzin and its mutant derivative tagged *N*-terminally with glutathione *S*-transferase (GST). Cells were grown in 1 L

of LB Broth medium (Sigma-Aldrich, Japan) at 37 °C to an OD_{610} of 1.0, and subjected to the induction of expression by the addition of 0.4 mM (final concentration) IPTG and cultured at 20°C for 16 h. After the induction, cells were harvested, washed with 50 mL of PBSE (137 mM NaCl, 27 mM KCl, 10 mM Na_2HPO_4, 1.8 mM KH_2PO_4, and 1 mM EDTA, pH 7.4), and pressed in 20 mL of PBSE containing cOmplete™, EDTA-free (Sigma-Aldrich, Japan) using a One Shot Model Cell disruption system (Constant Systems, UK). The sample was mixed with 0.1% (w/v, final concentration) Triton X-100, incubated at an ambient temperature for 10 min, and centrifuged at 2,000 x *g* at 4°C for 5 min. The supernatant fraction was retrieved and mixed with 1.5 mL of Glutathione Sepharose 4B resin (GE Healthcare, Japan) at an ambient temperature for 30 min. The resin was then washed with PBSE containing 0.1% (w/v) Triton X-100 and incubated with 7 mL of elution buffer [50 mM Tris-HCl, pH 7.6, 1 mM EDTA, 0.1% (w/v) Triton X-100, and 10 mM reduced glutathione] at an ambient temperature for 15 min. The eluted sample was dialyzed against 3 L of dialysis buffer [50 mM Tris-HCl, pH 7.6, 1 mM EDTA, and 0.1% (w/v) Triton X-100].

For the preparation of tag-free tafazzin, the purified GST-tagged tafazzin was treated with 320 U/ml (final concentration) of PreScission protease (GE Healthcare, Japan) in cleavage buffer (150 mM NaCl, 1 mM EDTA, 1 mM DTT, and 50 mM Tris-HCl, pH 7.6) at 4°C for 3 h. This reaction mixture was then applied to Glutathione Sepharose 4B resin (GE Healthcare) to obtain pure tag-free tafazzin. SDS-PAGE of purified GST-tagged and tag-free tafazzin and GST-tagged H77Q mutant were shown in supplemental Figure 8.

Preparation of Liposomes

Liposomes (large unilamellar vesicles) made of an acyl donor and acceptor mixture (PC/MLCL, PC/dilyso-CL (DLCL), or LPC/DLCL at a 9:1 molar ratio) were prepared by the extrusion method (*46*, *47*). Stock solutions of an acyl donor and acceptor in a methanol/chloroform (1:3, v/v) solution were mixed in the required proportion. A thin lipid film, which was obtained by evaporating organic solvents and was left under a vacuum overnight to remove residual organic solvents, was hydrated with Tris buffer (50 mM Tris-HCl, pH 7.4) and vortexed (final concentration of 9.0 mM choline, equivalent to 1.0 mM CL derivatives). After seven rounds of freeze-thawing under an N_2 atmosphere, the lipid suspension was extruded through a 100 nm pore polycarbonate filter using a LiposoFast device (Avestin, Ottawa, Canada). The diameter of liposomes was determined from dynamic light scattering

measurements (ELSZ-2Plus; Otsuka Electronic, Osaka, Japan). The particles scarcely varied in diameter with lipid compositions; the mean diameter estimated based on light scattering intensity was ~110 nm, as shown in supplemental Figure 9(A) taking PC(18:1-18:1)/*sn*-2'-MLCL(18:1-18:1/18:1-OH) liposomes (9:1 molar ratio) as an example. The concentrations of PCs in liposomal preparations were determined using an enzyme assay kit for choline (*47*) (Wako, Osaka, Japan).

Measurement of Transacylation Activity of Tafazzin in Liposomes

Isolated tafazzin (4.0 μg) was incubated with PC/MLCL, PC/DLCL, or LPC/DLCL liposomes in 85 μL of reaction buffer (50 mM Tris-HCl, pH 7.4) at 37°C, final lipids concentration being 0.59 mM. The final concentrations of Triton X-100, which was introduced into a reaction mixture with the enzyme, were maximally 0.08%. We confirmed by dynamic light scattering measurements that the particle size distribution of liposomes is maintained under the assay conditions, as shown in supplemental Figure 9(B) taking PC(18:1-18:1)/ *sn*-2'-MLCL(18:1-18:1/18:1-OH) liposomes (9:1 molar ratio) as an example.

The reaction was quenched after definite incubation periods by the addition of 5 μL of solvent A ($CH_3CN/H_2O/(C_2H_5)_3N/CH_3COOH$, 89:10:0.5:0.5 by vol.) and 5 μL of solvent B (2-propanol/H_2O/$(C_2H_5)_3N$/CH_3COOH, 89:10:0.5:0.5 by vol.). Note that the enzyme reaction was quenched within ~20 sec by this treatment. To accurately quantify lipid products, we directly subjected the reaction samples, without an extraction step using an organic solvent, to the HPLC analysis described below. The recovery of products in our HPLC analytical method was greater than 95%.

We adopted the reverse-phase ion-pair HPLC with acidified triethylamine to efficiently separate and quantify lipid products (*48*). HPLC analysis (SCL-10, Shimadzu, Japan) equipped with an evaporative light scattering detector (ELSD) (model 300S, Softa Co. USA) was performed in the gradient mobile phase using solvents A and B, as described above. The RP-18 GP Aqua 5 μm ODS column (150 × 4.6 mm, KANTO Chemical, Japan) was connected with the guard cartridge (5C18-AR-II, 10 × 4.6 mm, Nacalai Tesque, Japan), both of which were incubated at 50°C in the column oven. ELSD (58° and 72°C for the spray chamber and drift tube, respectively) was kept at a pressure of 1.4 bar (2.5 L/min) for nebulization gas (N_2). To separate lipids, except for DLCL, the gradient profile used was as follows: 0–10 min, an isocratic run with 53% of solvent B; 10–30 min, 53 to 100% of solvent B with a linear gradient; 30–40 min, an isocratic run with

100% of solvent B. Flow rates were 0.8 and 0.4 mL/min for 0–18 and 18–40 min, respectively. For the separation of DLCL species, the HPLC system was operated under isocratic conditions with 20% of solvent B for 20 min (flow rate, 0.8 mL/min). The amounts of the lipid products were estimated by interpolating the light scattering intensity to calibration plots (in a range of 3 to 40 μg) obtained with each synthetic standard sample. Since chromatographic behavior of Triton X-100 and tafazzin in the HPLC analysis was remarkably different from that of lipid products of interest, they did not interfere with the detection of lipid products.

We note that ELSD is a powerful tool for detecting lipids that have no strong chromophore (*49*, *50*). Based on our experience, the sensitivity of ELSD is markedly superior, by at least ~100-fold, to that of a UV-visible absorption detector (e.g. monitoring absorption at 205 nm) for the detection of lipids; accordingly, our HPLC analytical method enabled the reproducible detection of lipids at one-digit μg levels.

Acknowledgments: We thank the Kyoto University Nano Technology Hub in "Nanotechnology Platform Project", which is sponsored by the Ministry of Education, Culture, Sports, Science and Technology (MEXT), Japan, for allowing us access to the dynamic light scattering particle-size analyzer (ELSZ-2Plus, Otsuka Electronic).

Conflict of interest: The authors declare that they have no conflicts of interest with the contents of this article.

Author contributions: Specific contributions to this work are as follows, M. A., M. O., and H. M. designed the research; M. A., Y. H., E. T., Y. S., and M. O. performed the research; M. A., M. O., Y. S., and H. M. wrote the paper.

REFERENCES

1. Schlame, M. (2008) Cardiolipin synthesis for assembly of bacterial and mitochondrial membrane. *Biochem. Cell Biol.* **82**, 99-112
2. Osman, C., Voelker, D. R., and Langer, T. (2011) Making heads or tails of phospholipids in mitochondria. *J. Cell Biol.* **192**, 7-16
3. Koshkin, V., and Greenberg, M. L. (2000) Oxidative phosphorylation in cardiolipin-lacking yeast mitochondria. *Biochem. J.* **347**, 687-691
4. Claypool, S. M., McCaffery, J. M., and Koehler, C. M. (2006) Mitochondrial mislocalization and altered assembly of a cluster of Barth syndrome mutant tafazzins. *J. Cell Biol.* **174**, 379-390
5. Schug, Z. T., and Gottlieb, E. (2009) Cardiolipin acts as a mitochondrial signaling platform to launch apoptosis. *Biochim. Biophys. Acta* **1788**, 2022-2031
6. Chang, S. C., Heacock, P. N., Clancey, C. J., and Dowhan, W. (1998) The PEL1 gene (renamed PGS1) encodes the phosphatidylglycerophosphate synthase of *Saccharomyces cerevisiae*. *J. Biol. Chem.* **273**, 9829-9836
7. Kelly, B. L., and Greenberg, M. L. (1990) Characterization and regulation of phosphatidylglycerophosphate phosphatase in *Saccharomyces cerevisiae*. *Biochim. Biophys. Acta* **1046**, 144-150
8. Osman, C., Haag, M., Wieland, F. T., Brügger, B., and Langer, T. (2010) A mitochondrial phosphatase required for cardiolipin biosynthesis: the PGP phosphatase Gep4. *EMBO J.* **29**, 1976-87
9. Zhang, J., Guan, Z., Murphy, A. N., Wiley, S. E., Perkins, G. A., Worby, C. A., Engel, J. L., Heacock, P., Nquyen, O. K., Wang, J. H., Raetz, C. R., Dowhan, W., and Dixon, J. E. (2011) Mitochondrial phosphatase PTPMT1 is essential for cardiolipin biosynthesis. *Cell Metab.* **13**, 690-700
10. Chang, S. C., Heacock, P. K., Mileykovskaya, E., Voelker, D. R., and Dowhan, W. (1998) Isolation and characterization of the gene (CLS1) encoding cardiolipin synthase in *Saccharomyces cerevisiae*. *J. Biol. Chem.* **273**, 14933-14941
11. Tuller, G., Hrastnik, C., Achleitner, G., Schiefthaler, U., Klein, F., and Daum, G. (1998) YDL142c encodes cardiolipin synthase (Cls1p) and is non-essential for aerobic growth of *Saccharomyces cerevisiae*. *FEBS Lett.* **421**, 15-18
12. Gallet, P. F., Petit, J. M., Maftah, A., Zachowski, A., and Julien, R. (1997) Asymmetrical distribution of cardiolipin in yeast inner mitochondrial membrane triggered by carbon catabolite repression.

Biochem. J. **324**, 627-634

13. Xu, Y., Kelley, R. I., Blanck, T. J., and Schlame, M. (2003) Remodeling of cardiolipin by phospholipid transacylation. *J. Biol. Chem.* **278**, 51380-51385
14. Beranek, A., Rechberger, G., Knauer, H., Wolinski, H., Kohlwein, S. D., and Leber, R. (2009) Identification of a cardiolipin-specific phospholipase encoded by the gene CLD1 (YGR110W) in yeast. *J. Biol. Chem.* **284**, 11572-11578
15. Taylor W. A. and Hatch, G. M. (2009) Identification of the human mitochondrial linoleoyl-coenzyme A monolysocardiolipin acyltransferase (MLCL AT-1). *J. Biol. Chem.* **284**, 30360-30371
16. Cao, J., Liu, Y., Lockwood, J., Burn, P., and Shi, Y. (2004) A novel cardiolipin-remodeling pathway revealed by a gene encoding an endoplasmic reticulum-associated acyl-CoA:lysocardiolipin acyltransferase (ALCAT1) in mouse. *J. Biol. Chem.* **279**, 31727-31734
17. Xu, Y., Malhotra, A., Ren, M., and Schlame, M. (2006) The enzymatic function of tafazzin. *J. Biol. Chem.* **281**, 39217-39224
18. Barth, P. G., Scholte, H.R., Berden, J. A., Van der Klei-Van Moorsel, J. M., Luyt-Houwen, I. E., Van't Veer-Korthof, E. T., Van der Harten, J. J., and Sobotka-Plojhar, M. A. (1983) An X-linked mitochondrial disease affecting cardiac muscle, skeletal muscle and neutrophil leucocytes. *J. Neurol. Sci.* **62**, 327-355
19. Bione, S., D'Adamo, P., Maestrini, E., Gedeon, A. K., Bolhuis, P. A., and Toniolo, D. (1996) A novel X-linked gene, G4.5. is responsible for Barth syndrome. *Nat. Genet.* **12**, 385-389
20. Gu, Z., Valianpour, F., Chen, S., Vaz, F. M., Hakkaart, G. A., Wanders, R. J., and Greenberg, M. L. (2004) *Mol. Microbiol.* **51**, 149-158
21. Valianpour, F., Mitsakos, V., Schlemmer, D., Towbin, J. A., Taylor, J. M., Ekert, P.G., Thorburn, D.R., Munnich, A., Wanders, R. J., Barth, P. G., and Vaz, F. M. (2005) Monolysocardiolipins accumulate in Barth syndrome but do not lead to enhanced apoptosis. *J. Lipid Res.* **46**, 1182-1195
22. Xu, Y., Condell, M., Plesken, H., Edelman-Novemsky, I., Ma, J., Ren, M., and Schlame, M. (2006) A *Drosophila* model of Barth syndrome. *Proc. Natl. Acad. Sci. U.S.A.* **103**, 11584-11588
23. Whited, K., Baile, M. G., Currier, P., and Claypool, S. M. (2013) Seven functional classes of Barth syndrome mutation. *Hum. Mol. Genet.* **22**, 483-492
24. Malhotra, A., Xu, Y., Ren, M., and Schlame, M. (2009) Formation of molecular species of mitochondrial cardiolipin. 1. A novel transacylation mechanism to shuttle fatty acids between *sn*-1 and *sn*-2 positions of multiple phospholipid species. *Biochim. Biophys. Acta* **1791**, 314-320

25. Schlame, M, Ren, M., Xu, Y., Greenberg, M. L., and Haller, I. (2005) Molecular symmetry in mitochondrial cardiolipins. *Chem. Phys. Lipids* **138**, 38-49
26. Schlame, M., Acehan, D., Berno, B., Xu, Y., Valvo, S., Ren, M., Stokes, D. L., and Epand, R. M. (2012) The physical state of lipid substrates provides transacylation specificity for tafazzin. *Nat. Chem. Biol.* **8**, 862-869
27. Schlame, M. (2013) Cardiolipin remodeling and the function of tafazzin. *Biochim. Biophys. Acta* **1831**, 582-588
28. Renner, L. D., and Weibel, D. B. (2011) Cardiolipin microdomains localize to negatively curbed regions of *Escherichia coli* membranes. *Proc. Natl. Acad. Sci. U.S.A.,* **108**, 6264-6269
29. Schlame, M. (2008) Cardiolipin synthesis for the assembly of bacterial and mitochondrial membranes. *J. Lipid Res.* **49**, 1607-1620
30. Epand, R. M., D'Souza, K., Bemo, B., and Schlame, M. (2015) Membrane curvature modulation of protein activity determined by NMR. *Biochim. Biophys. Acta* **1848**, 220-228
31. Abe, M., Kitsuda, S., Ohyama, S., Koubori, S., Murai, M., and Miyoshi, H. (2010) Concise procedure for the synthesis of cardiolipins having different fatty acid combinations. *Tetrahedron Lett.* **51**, 2071-2073.
32. Abe, M., Niibayashi, R., Koubori, S., Moriyama, I., and Miyoshi, H. (2011) Molecular mechanisms for the induction of peroxidase activity of the cytochrome *c*-cardiolipin complex. *Biochemistry*, **50**, 8383-8391
33. Abe, M., Nakano, M., Kosaka, A., and Miyoshi, H. (2015) Syntheses of cardiolipins for a photoaffinity labeling study. *Tetrahedron Lett.* **56**, 2258-2261.
34. Rytömaa, M., and Kinnunen, P. K. J. (1994) Evidence for two distinct acidic phospholipid-binding sites in cytochrome *c*. *J. Biol. Chem.* **269**, 1770-1774
35. Rytömaa, M., and Kinnunen, P. K. J. (1995) Reversibility of the binding of cytochrome *c* to liposomes. *J. Biol. Chem*. **270**, 3197-3202
36. Jiang, G., Xu, Y., and Prestwich, G. D. (2006) Practical enantiospecific syntheses of lysobiphosphatidic acid and its analogues. *J. Org. Chem.* **71**, 934-939
37. Rosseto, R. Bibak, N., DeOcampo, R., Shah, T., Gabrielian, A., and Hajdu, J. (2007) A new synthesis of lysophosphatidylcholines and related derivatives. Use of *p*-toluenesulfonate for hydroxyl group protection. *J. Org. Chem.* **72**, 1691-1698
38. Claypool, S. M., Whited, K., Srijumnonq, S., Han, X., and Koehler, C. M. (2011) Barth syndrome

mutations that cause tafazzin complex lability. *J. Cell. Biol.* **192**, 447-462

39. Butterworth, P. J., Warren, F. J., Grassby, T., Patel, H., and Ellis, P. R. (2012) Analysis of starch amylolysis using plots for first-order kinetics. *Carbohydrate Polymers* **87**, 2189-2197
40. Baile, M. G., Sathappa, M., Lu, Y. W., Pryce, E., Whited, K., McCaffery, J. M., Han, X., Alder, N. N., and Claypool, S. M. (2014) Unremodeled and remodeled cardiolipin are functionally indistinguishable in yeast. *J. Biol. Chem.* **289**, 1768-1778
41. Kiebish, M. A., Yang, K., Liu, X., Mancuso, D. J., Guan, S., Zhao, Z., Sims, H. F., Cerqua, R., Cade, W. T., Han, X., and Gross, R. W. (2013) Dysfunctional cardiac mitochondrial bioenergetic, lipidomic, and signaling in a murine model of Barth syndrome. *J. Lipid Res*. **54**, 1312-1325
42. Lu, Ya-Wen., Galbraith, L., Herndon, J. D., Lu, Ya-Lin., Pras-Raves, M., Vervaart, M., Kampen, A. V., Luyf, A., Koehler, C. M., McCaffery, J. M., Gottlieb, E., Vaz, F. M., and Claypool, S. M. (2016) Defining functional classes of Barth syndrome mutation in humans. *Hum. Mol. Genet.* DOI: 10.1093/hmg/ddw046.
43. Ren, M., Phoon, C. K. L., and Schlame, M. (2014) Metabolism and function of mitochondrial cardiolipin. *Prog. Lipid Res*. *55*, 1-16
44. Ye, C., Lou, W., Li, Y., Chatzispyrou, I. A., Hüttemann, M., Lee, I., Houtkooper, R. H., Vaz, F. M., Chen, S., and Greenberg, M. L. (2014) Deletion of the cardiolipin-specific phospholipase Cld1 rescues growth and life span defects in the tafazzin mutant: implications for Barth syndrome. *J. Biol. Chem.* **289**, 3114-3125
45. Baile, M. G., Whited, K., and Claypool, S. M. (2013) Deacylation on the matrix side of the mitochondrial inner membrane regulates cardiolipin remodeling. *Mol. Biol. Cell* **24**, 2008-2020
46. Shintou, K., Nakano, M., Kamo, T., Kuroda, Y., and Handa, T. (2007) Interaction of an amphipathic peptide with phosphatidylcholine/phosphatidylethanolamine mixed membrane. *Biophys. J.* **93**, 3900-3906
47. Nakano, M., Fukuda, M., Kudo, T., Matsuzaki, N., Azuma, T., Sekine, K., Endo, H., and Handa, T. (2009) Fli p-flop of phospholipids in vesicles: Kinetic analysis with time-resolved small-angle neutronscattering. *J. Phys. Chem. B,* **113**, 6745-6748.
48. Minkler, P. E. and Hoppel, C. L. (2010) Separation and characterization of cardiolipin molecular species by reverse-phase ion pair high-performance liquid chromatography-mass spectrometry. *J. Lipid Res*. **51**, 856-865
49. Yamashita, S., Abe, A., Nakagawa, K., Kinoshita, M., and Miyazawa, T. (2014) Separation and

detection of plasmalogen in marine invertebrates by high-performance liquid chromatography with evaporative light-scattering detection. *Lipids* **49**, 1261–1273

50. Oswalda, M., Platscherb, M., Geisslera, S., and Goepferichc, A. (2016) HPLC analysis as a tool for assessing targeted liposome composition. *Int. J. Pharm*. **497**, 293–300

FOOTNOTES

This study was supported by a Grant-in-Aid for Scientific Research (Grant 26292060 to H. M. and Grant 26450139 to M. A.) from the Japan Society for the Promotion of Science.

The abbreviations used are: CL, cardiolipin; DLCL, dilyso-cardiolipin; ELSD, evaporative light scattering detector; GST, glutathione *S*-transferase; HPLC, high performance liquid chromatography; LC-MS, liquid chromatography-mass spectrometry; LPC, lyso-phosphatidylcholine; MBP, maltose-binding protein; MLCL, monolyso-cardiolipin; PC, phosphatidylcholine; PE, phosphatidylethanolamine.

FIGURE LEGENDS

Figure 1

Structures of CL, monolyso-CL (MLCL), dilyso-CL (DLCL), and PC species synthesized in this study. The synthetic procedures for these phospholipids are described in Supplemental Data. Regarding the abbreviated designation of CL species, four acyl chains are arranged to make the chiral carbon of the central glycerol to have the *R* configuration. For MLCL species, the synthetic products are racemic mixtures of (*S*) *sn*-1- and (*R*) *sn*-1'-MLCL or (*S*) *sn*-2- and (*R*) *sn*-2'-MLCL. Similarly, one of DLCL species is a racemic mixture of (*R*) *sn*-1/*sn*-2'- and (*S*) *sn*-1'/*sn*-2-DLCL.

Figure 2

Effects of GST-tag, Ca^{2+}, or a point mutation on the catalytic activity of tafazzin. Liposomal membranes were prepared from a mixture of PC(18:1-18:1) and *sn*-2'-MLCL(18:1-18:1/18:1-OH) at a 9:1 molar ratio (total of 10 mM lipids). The reaction buffer (85 μL) contained 50 nmol of total lipids (a final lipid concentration of 0.59 mM). The reaction was started by the addition of purified GST-tagged tafazzin at final concentration of 4.0 μg/mL, except column *b* (2.5 μg/mL for tag-free tafazzin). The production of CL(18:1-18:1/18:1-18:1) was determined after 40 min incubation. Column *a*; transacylation catalyzed by GST-tagged tafazzin, column *b*; transacylation catalyzed by tag-free tafazzin, column *c*; transacylation catalyzed by GST-tagged tafazzin in the presence of 1 mM Ca^{2+}, column *d*; transacylation catalyzed by GST-tagged tafazzin in the presence of 20 mM Ca^{2+}, column *e*; transacylation catalyzed by H77Q mutant. For the assay of H77Q mutant, liposomes were prepared from a mixture of PC(18:2-18:2) and *sn*-2'-MLCL(18:1-18:1/18:1-OH) at a 9:1 molar ratio. The control (GST-tagged wild-type tafazzin)

activity in this transacylation was 3.6 (± 0.2) nmol of CL(18:1-18:1/18:1-18:2). Data shown are mean values ± S.D. (n = 3).

Figure 3

Discrimination of *sn*-1-LPC and *sn*-2-LPC isomers. (A) HPLC (detected by ELSD) analysis of (i) *sn*-1-LPC(OH-18:1) alone (1.2 μg), (ii) *sn*-2-LPC(18:1-OH) alone (1.0 μg), and (iii) a reaction mixture after 40 min incubation in the presence of tafazzin. Note that weak light scattering around 30 min observed for the reaction mixture arose from impurities; the scattering intensities did not change with time. (B) ESI-LC/MS (detected by a selected ion monitoring mode, m/z 522.4) analysis of (i) *sn*-1-LPC(OH-18:1) alone (1.2 μg), (ii) *sn*-2-LPC(18:1-OH) alone (1.2 μg), and (iii) a reaction mixture after 40 min incubation in the presence of tafazzin. HPLC (ELSD) analysis was performed according to the procedure described in the Experimental Procedures, except that solvents A (H_2O containing 0.1% formic acid) and B (100% MeOH) were used as mobile phase (flow rate was 0.4 mL/min). The gradient profile used was as follows: 0–20 min, 60 to 90% of solvent B with a linear gradient; 20–40 min, an isocratic run with 100% of solvent B. ESI-LC/MS analysis was performed using triple quadrupole LCMS-8040 (Shimadzu, Japan) instrument with electrospray ionization in positive mode (DL 250°C; nebulizing gas 3.0 L/min; heat block 250°C; drying gas 15 L/min). The LC conditions were identical with those set for HPLC (ELSD) analysis.

Figure 4

Tafazzin-mediated acyl transfer from PC to *sn*-2-MLCL. Liposomal membranes were prepared from a mixture of PC(18:1-18:1) or PC(18:2-18:2) and *sn*-2'-MLCL(18:1-18:1/18:1-OH) at a 9:1 molar ratio (total of 10 mM lipids). The reaction buffer (85 μL) contained 50 nmol of total lipids (a final lipid concentration of 0.59 mM). The reaction was started by the addition of purified GST-tagged tafazzin at final concentration of 4.0 μg/mL. (A) The time-course for the production of CL(18:1-18:1/18:1-18:1) (*closed circles*) or CL(18:1-18:2/18:1-18:1) (*open circles*) was shown. Data shown are mean values ± S.D. (n = 4). (B) The reaction rate constant (k) for the reaction [PC(18:2-18:2) + *sn*-2'-MLCL(18:1-18:1/18:1-OH) → LPC(18:2-OH) + CL(18:1-18:2/18:1-18:1)] was estimated by a modified Guggenheim plot (*39*).

Figure 5

Discrimination of *sn*-1-MLCL and *sn*-2-MLCL isomers. (A) ^{1}H NMR [400 MHz, $CDCl_3$:CD_3OD = 1:1 (*v*/*v*)] spectra of *sn*-1'-MLCL(18:1-18:1/OH-18:1). An integration ratio of H(8):H(2) indicates that the content of *sn*-2 isomer was less than 5%. (B) ^{1}H NMR [400 MHz, $CDCl_3$:CD_3OD = 1:1 (*v*/*v*)] spectra of *sn*-2'-MLCL(18:1-18:1/18:1-OH). (C) HPLC analysis (detected by ELSD) of (i) *sn*-1'-MLCL(18:1-18:1/OH-18:1) alone (5.0 μg), (ii) *sn*-2'-MLCL(18:1-18:1/18:1-OH) alone (5.0 μg), and (iii) a mixture of them (5.0 μg each). Detailed HPLC analytical conditions were described in Experimental Procedures.

Figure 6

Tafazzin-mediated acyl transfer from *sn*-2-MLCL to *sn*-2-LPC. Lipid dispersions were prepared from a mixture of *sn*-2'-MLCL(18:1-18:1/18:1-OH) and *sn*-2-LPC(18:1-OH) at a 1:9 molar ratio (total of 10 mM lipids). The reaction buffer (85 μL) contained 50 nmol of total lipids (a final lipid concentration of 0.59 mM). The reaction was started by the addition of purified GST-tagged tafazzin at a final concentration of 4.0 μg/mL. The time-courses for the consumption and production of *sn*-2-MLCL (*closed circles*) and PC(18:1-18:1) (*open circles*), respectively, were shown. Data shown are mean values ± S.D. (*n* = 3).

Figure 7

Tafazzin-mediated acyl transfer from PC to *sn*-2/*sn*-2'-DLCL. Liposomal membranes were prepared from a mixture of PC(18:1-18:1) and *sn*-2/*sn*-2'-DLCL(18:1-OH/18:1-OH) at a 9:1 molar ratio (total of 10 mM lipids). The reaction buffer (85 μL) contained 50 nmol of total lipids (a final lipid concentration of 0.59 mM). The reaction was started by the addition of purified GST-tagged tafazzin at a final concentration of 4.0 μg/mL. (A) The time-courses for the production of *sn*-2'-MLCL(18:1-18:1/18:1-OH) (*open circles*) and CL(18:1-18:1/18:1-18:1) (*closed circles*) were shown. (B) In order to monitor the production of CL(18:1-18:1/18:1-18:1), the incubation period was elongated. Data shown are mean values ± S.D. (*n* = 3).

Figure 8

Purification of recombinant yeast tafazzin and its mutant derivative (H77Q). Each of the purified samples (equivalent to ~1 μg protein) was applied to SDS-PAGE (10% acrylamide, 0.1% SDS), and stained with Coomassie Brilliant Blue solution. Lane 1: GST-tagged wild-type tafazzin, lane 2:

GST-tagged mutant (H77Q), lane 3: tag-free wild-type tafazzin. The indications of molecular weight are also shown.

Figure 9

The particle size distribution profiles of liposomes determined by dynamic light scattering measurements. Dynamic light scattering measurements (ELSZ-2Plus; Otsuka Electronic, Japan) were performed at 37°C immediately after the preparation of liposomes, which were composed of PC(18:1-18:1) and *sn*-2'-MLCL(18:1-18:1/18:1-OH) at a 9:1 molar ratio (A) and during the incubation in a reaction buffer in the presence of tafazzin (4.0 μg/mL) (B). The particle size distribution profiles were estimated based on light scattering intensity (i) or particle numbers (ii); the profiles depend on how the measured data are weighted: by scattering intensity or by numbers.

TABLE 1

The rate constant (k, min^{-1}) for *S. cerevisiae* tafazzin-mediated transacylation from PC to monolyso-CL (mean values ± SD, n = 3–4).

Acyl Acceptors / Acyl Donors	Monolyso-CL(18:1)$_3$		Monolyso-CL(18:2)$_3$	
	sn-1'-OH	*sn*-2'-OH	*sn*-1'-OH	*sn*-2'-OH
PC(18:1-18:1)	0.062 (± 0.006)	0.075 (± 0.010)	0.084 (± 0.011)	0.066 (± 0.005)
PC(18:2-18:2)	0.099 (± 0.006)	0.098 (± 0.008)	0.13 (± 0.02)	0.097 (± 0.008)
PC(16:0-16:0)	N.E.[a]	N.E.	–[b]	–
PC(16:1-16:1)	0.081 (± 0.003)	0.068 (± 0.005)	–	–

a) Not estimated because the amounts of CL produced after a 40 min reaction were less than 0.3 nmol.

b) Not examined.

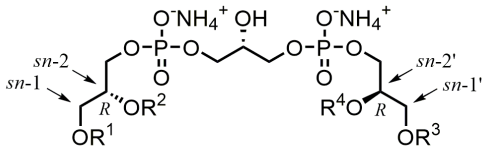

CLs

CL(18:1-18:1/18:1-18:1): R^1– R^4 = oleoyl
CL(18:2-18:2/18:2-18:2): R^1– R^4 = linoleoyl
CL(16:0-16:0/16:0-16:0): R^1– R^4 = palmitoyl
CL(18:2-18:1/18:1-18:1): R^1 = linoleoyl; R^2– R^4 = oleoyl
CL(18:1-18:2/18:1-18:1): R^1, R^3, R^4 = oleoyl; R^2 = linoleoyl
CL(18:2-18:2/18:2-18:1): R^1– R^3 = linoleoyl; R^4 = oleoyl
CL(18:2-18:2/18:1-18:2): R^1, R^2, R^4 = linoleoyl; R^3 = oleoyl
CL(18:1-18:1/18:1-16:0): R^1– R^3 = oleoyl; R^4 = palmitoyl
CL(18:1-18:1/16:0-18:1): R^1, R^2, R^4 = oleoyl; R^3 = palmitoyl
CL(18:1-18:1/18:1-16:1): R^1– R^3 = oleoyl; R^4 = palmitoleoyl
CL(18:1-18:1/16:1-18:1): R^1, R^2, R^4 = oleoyl; R^3 = palmitoleoyl

MLCLs

sn-1-MLCL(18:1-18:1/OH-18:1): R^1, R^2, R^4 = oleoyl; R^3 = H
sn-1-MLCL(18:2-18:2/OH-18:2): R^1, R^2, R^4 = linoleoyl; R^3 = H
sn-2-MLCL(18:1-18:1/18:1-OH): R^1– R^3 = oleoyl; R^4 = H
sn-2-MLCL(18:2-18:2/18:2-OH): R^1– R^3 = linoleoyl; R^4 = H

DLCLs

sn-1/*sn*-1'-DLCL(OH-18:1/OH-18:1): R^1, R^3 = H; R^2, R^4 = oleoyl
sn-1/*sn*-2'-DLCL(OH-18:1/18:1-OH): R^1, R^4 = H; R^2, R^3 = oleoyl
sn-2/*sn*-2'-DLCL(18:1-OH/18:1-OH): R^1, R^3 = oleoyl; R^2, R^4 = H

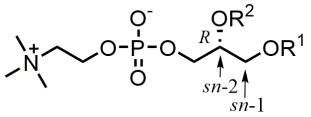

PCs

PC(18:1-16:0): R^1 = oleoyl; R^2 = palmitoyl
sn-1-LPC(OH-18:1): R^1 = H; R^2 = oleoyl
sn-2-LPC(18:1-OH): R^1 = oleoyl; R^2 = H

Figure 1

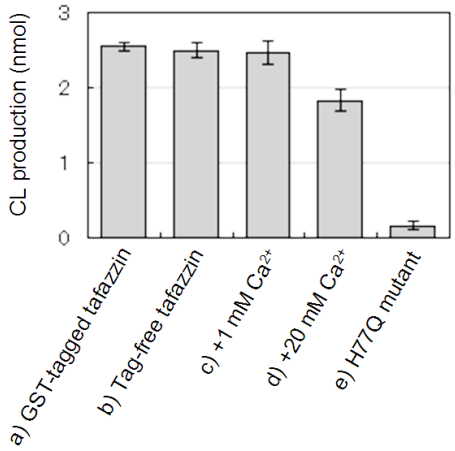

Figure 2

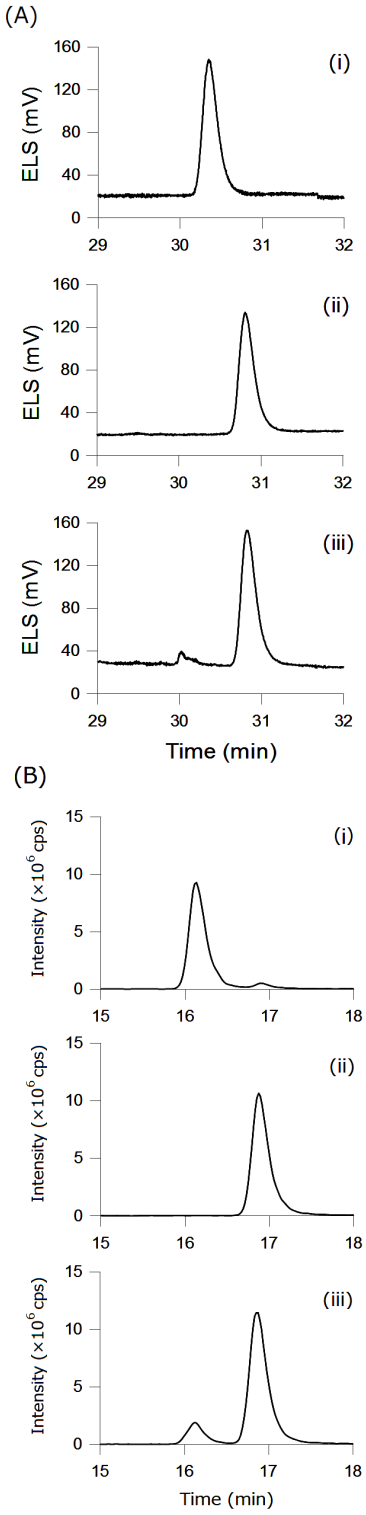

Figure 3

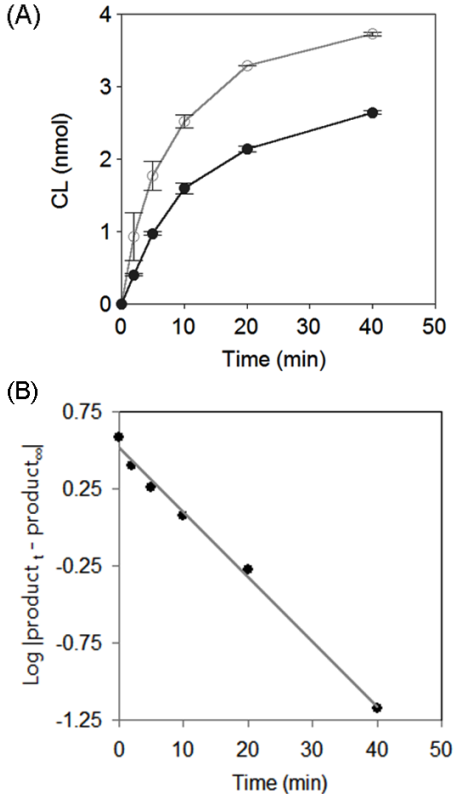

Figure 4

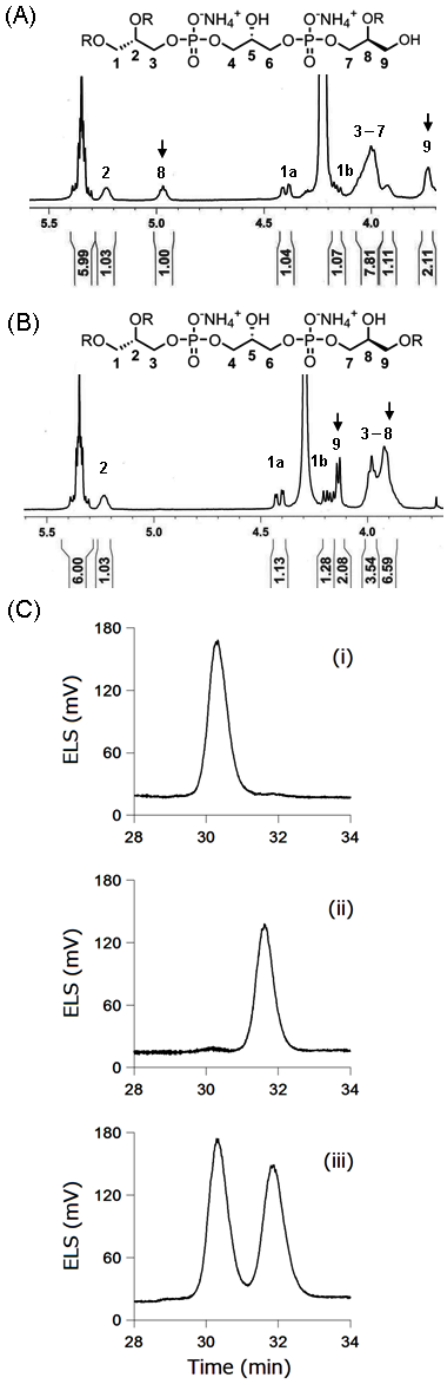

Figure 5

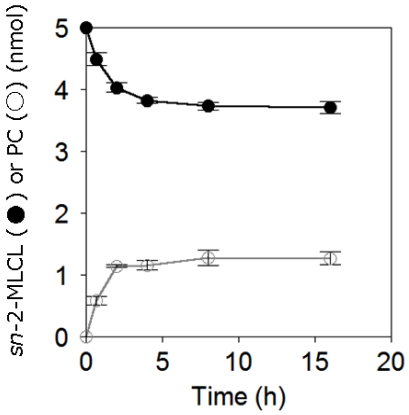

Figure 6

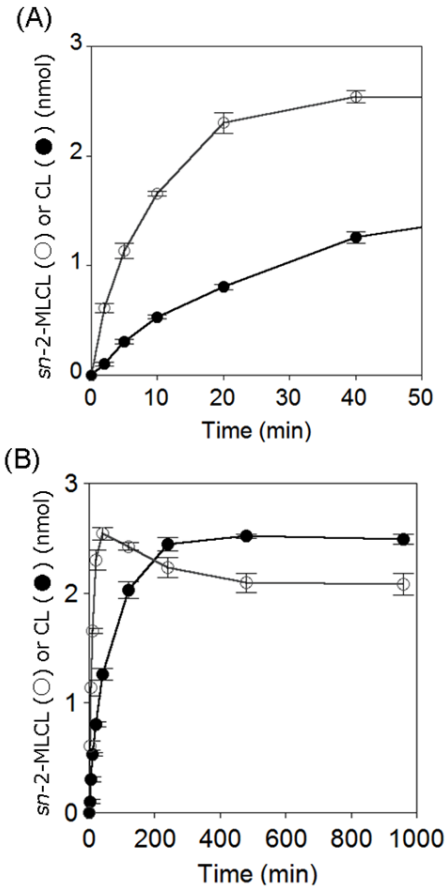

Figure 7

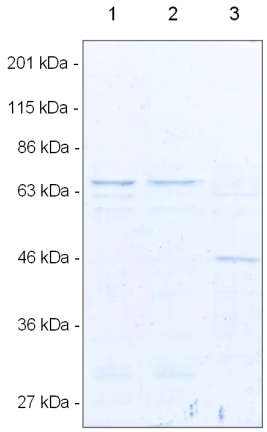

Figure 8

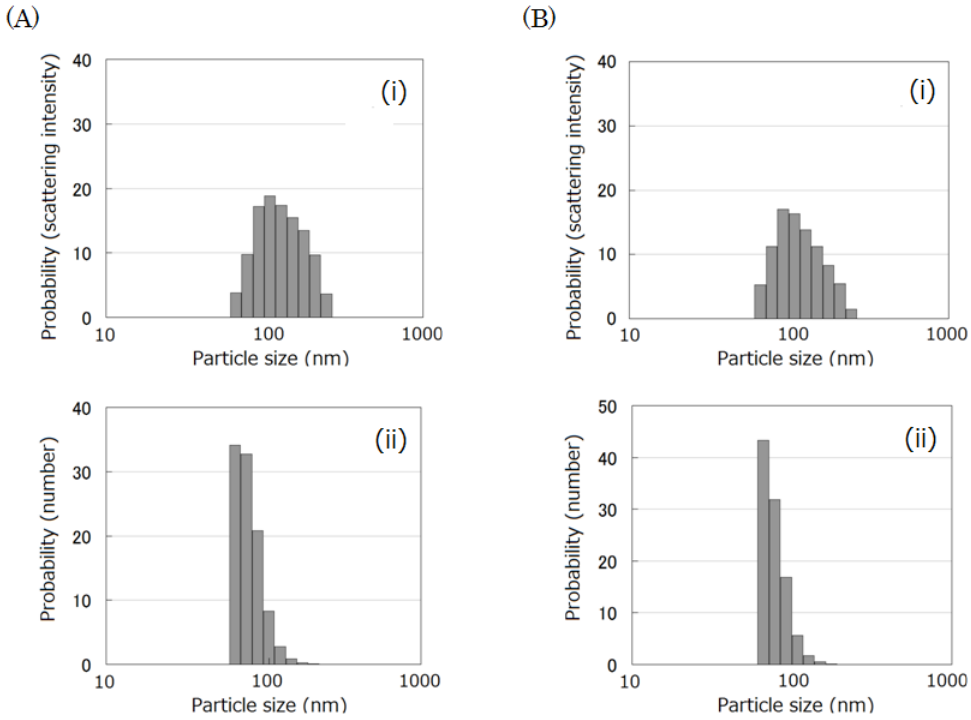

Figure 9

Supplemental Data

Mechanism for remodeling of the acyl chain composition of cardiolipin catalyzed by *Saccharomyces cerevisiae* tafazzin

Masato Abe, Yui Hasegawa, Masahide Oku, Yoshiki Sawada, Eriko Tanaka, Yasuyoshi Sakai, and Hideto Miyoshi

Syntheses of CL, MLCL, DLCL, and PC species

General procedures

^{1}H NMR spectra were recorded at 400 or 500 MHz with a Bruker AVANCE 400 or AVANCE 500, respectively, using tetramethylsilane (TMS) as an internal standard. ^{13}C NMR spectra were recorded at 100 or 125 MHz. Chemical shift (δ) were given in ppm relative to TMS. The ESI-MS were recorded with a Shimadzu LCMS-8040. Thin layer chromatography was performed on Merk TLC Plate Silica gel 60 F254, and the spot was detected by anisaldehyde, moribdenephosphate, iodine or UV absorption. Dry solvents were either used as purchased or freshly distilled using common practices where appropriate. Column chromatography were performed on Woko-gel C200.

Abbreviations

DCC, *N,N'*-dicyclohexylcarbodiimide; DDQ, 2,3-dichloro-5,6-dicyano-*p*-benzoquinone; DMAP, 4-dimethylaminopiridine; OMe, methoxy; PMB, *p*-methoxybenzyl; MeOP[N(*i*Pr$_2$)]$_2$, methyl *N,N,N',N'*-tetraisopropylphosphoramidite; r.t., room temperature; TEA, trimethylamine; THF, tetrahydrofuran; TMA, trimethylamine

Outline of synthetic procedures

Scheme 1

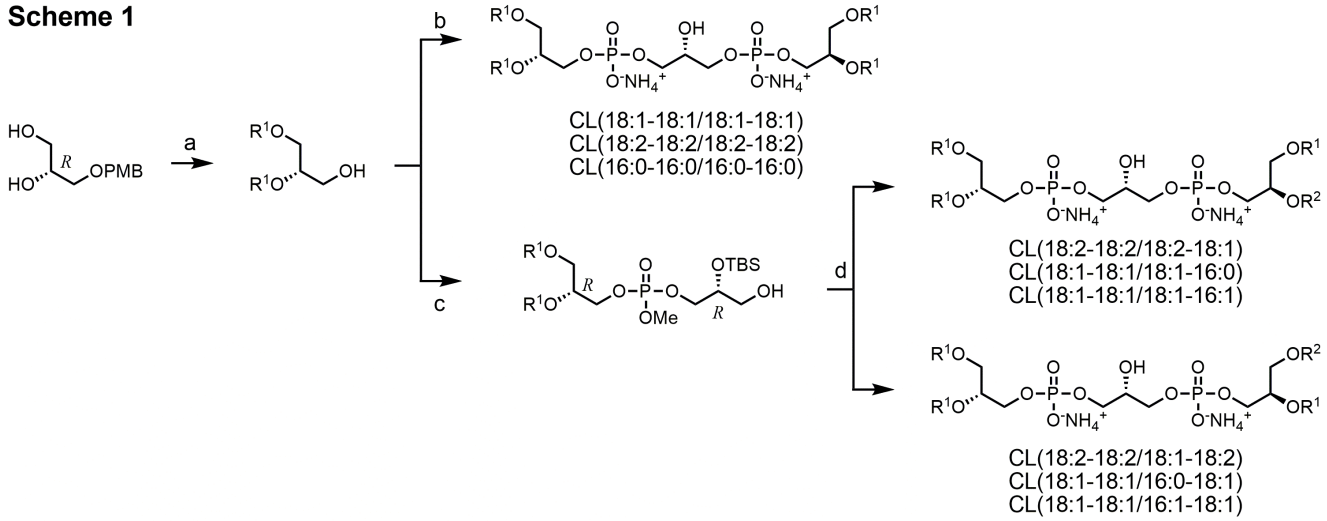

Reagents and conditions: (**a**) i) R^{1}OH, DCC, DMAP, ii) DDQ, CH_2Cl_2/H_2O (20:1); (**b**) i) MeOP[N(*i*Pr)$_2$]$_2$, 1*H*-tetrazole (0.5 eq), MS 4A, ii) 1*H*-tetrazole (3 eq), (*R*)-$HOCH_2CH(OTBS)CH_2OH$, iii) Bu_4NIO_4, iv) 45% aq. TMA/CH_2Cl_2/CH_3CN/*i*PrOH (4/2/3/3; v/v), v) HCl, THF, then aq. NH_4OH; (**c**) i) MeOP[N(*i*Pr)$_2$]$_2$, 1*H*-tetrazole (0.5 eq), MS 4A, ii) 1*H*-tetrazole (3 eq), (*R*)-$HOCH_2CH(OTBS)CH_2OTBS$, iii) Bu_4NIO_4, iv) HF-pyridine, THF; (**d**) i) MeOP[N(*i*Pr)$_2$]$_2$, 1*H*-tetrazole (0.5 eq), MS 4A, ii) 1*H*-tetrazole (3 eq), (*R*)-$HOCH_2CH(OR^2)CH_2OR^1$ or (*R*)-$HOCH_2CH(OR^1)CH_2OR^2$, iii) Bu_4NIO_4, iv) 45% aq. TMA/CH_2Cl_2/CH_3CN/*i*PrOH (4/2/3/3; v/v), v) HCl, THF, then aq. NH_4OH.

(Continued)

Scheme 2

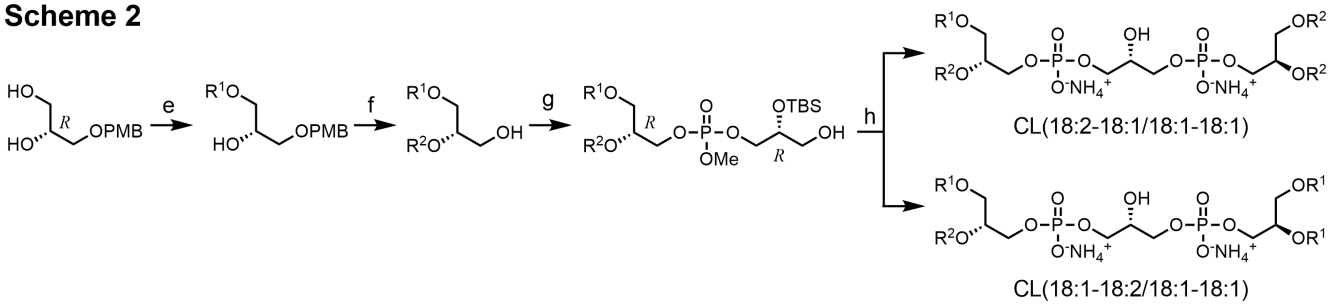

Scheme 3

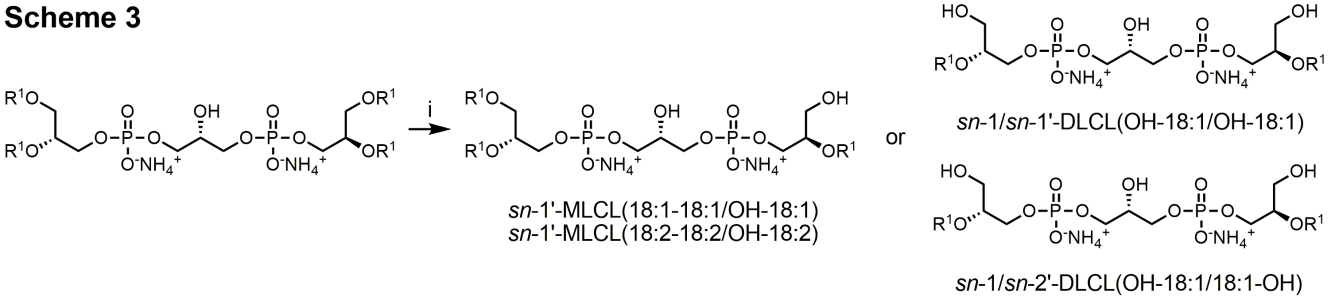

Scheme 4

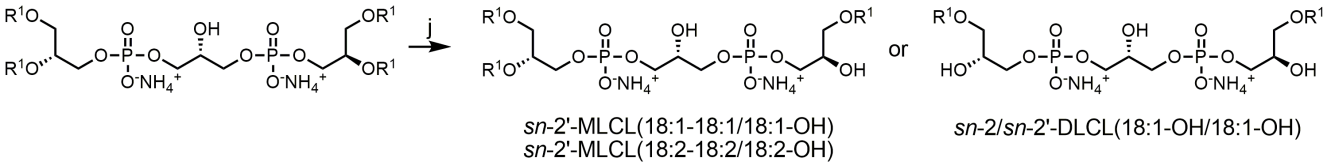

Scheme 5

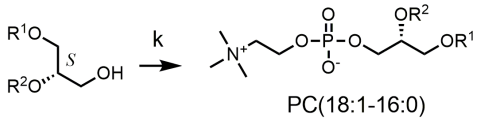

Scheme 6

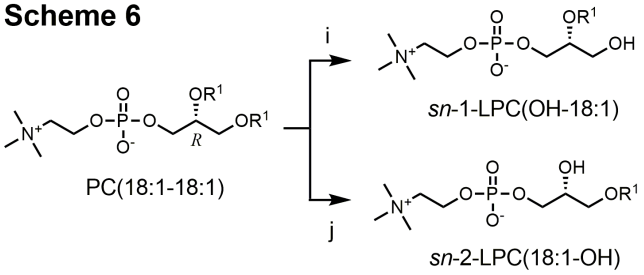

Reagents and conditions: (**e**) R^1OH (0.4 eq), DCC, DMAP; (**f**) i) R^2OH, DCC, DMAP, ii) DDQ, CH_2Cl_2/H_2O (20:1); (**g**) i) $MeOP[N(iPr)_2]_2$, 1*H*-tetrazole (0.5 eq), MS 4A, ii) 1*H*-tetrazole (3 eq), (*R*)-$HOCH_2CH(OTBS)CH_2OTBS$, iii) Bu_4NIO_4, iv) HF-pyridine, THF; (**h**) i) $MeOP[N(iPr)_2]_2$, 1*H*-tetrazole (0.5 eq), MS 4A, ii) 1*H*-tetrazole (3 eq), (*R*)-$HOCH_2CH(OR^1)CH_2OR^1$ or (*R*)-$HOCH_2CH(OR^2)CH_2OR^2$, iii) Bu_4NIO_4, iv) 45% aq. TMA/CH_2Cl_2/CH_3CN/*i*PrOH (4/2/3/3; v/v), v) HCl, THF, then aq. NH_4OH; (**i**) porcine phospholipase A_2, $CaCl_2$, MeOH; (**j**) *Mucor javanics* lipase, Triton X-100, boric acid-borax buffer; (**k**) i) $MeOP[N(iPr)_2]_2$, 1*H*-tetrazole (0.5 eq), MS 4A, ii) 1*H*-tetrazole (3 eq), choline tosylate, iii) Bu_4NIO_4, iv) 45% aq. TMA/CH_2Cl_2/CH_3CN/*i*PrOH (4/2/3/3; v/v).

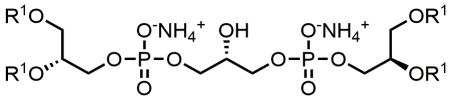

CL(18:1-18:1/18:1-18:1) (R^1: oleoyl)

CL(18:1-18:1/18:1-18:1) was synthesized according to the previous method (Scheme 1, refs. 1 and 2): ^{1}H NMR (400 MHz, CD_3OD:$CDCl_3$ = 1:1): δ 5.19 (m, 8H), 5.18 (m, 2H), 4.23 (dd, 2H, *J* = 12.0, 3.0 Hz), 4.02 (dd, 2H, *J* = 12.0, 6.8 Hz), 3.88-3.72 (m, 9H), 2.18 (t, 4H, *J* = 7.8 Hz), 2.16 (t, 4H, *J* = 7.8 Hz), 1.87 (m, 16H), 1.45 (m, 9H), 1.24-1.05 (m, 80H), 0.73 (t, 12H, *J* = 6.6 Hz); ^{13}C NMR (100 MHz, CD_3OD:$CDCl_3$ = 1:1): δ 174.87 (2C), 174.57 (2C), 131.01 (4C), 130.66 (2C), 130.64 (2C), 71.43 (2C), 70.56, 66.71 (2C), 64.71 (2C), 63.70 (2C), 35.19 (2C), 35.05 (2C), 32.90 (4C), 30.75 (8C), 30.71 (2C), 30.51 (2C), 30.30 (8C), 30.26 (2C), 30.19 (2C), 30.17 (2C), 30.15 (2C), 30.12 (2C), 29.97 (2C), 28.20 (8C), 25.90 (2C), 25.84 (2C), 23.65 (4C), 14.98 (4C); ESI-MS (m/z): 727.8 $[M-2NH_4]^{2-}$, 1456.0 $[M-2NH_3-H]^-$.

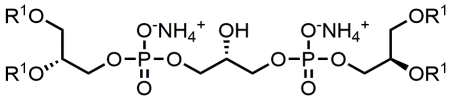

CL(18:2-18:2/18:2-18:2) (R^1: linoleoyl)

CL(18:2-18:2/18:2-18:2) was synthesized according to the previous method (Scheme 1, refs. 1 and 2): ^{1}H NMR (400 MHz, CD_3OD:$CDCl_3$ = 1:1): δ 5.34 (m, 16H), 5.25 (m, 2H), 4.45 (dd, 2H, *J* = 12.0, 4.0 Hz), 4.20 (dd, 2H, *J* = 12.0, 6.7 Hz), 4.00 (t, 4H, *J* = 5.6 Hz), 3.92 (m, 5H), 2.77 (t, 8H, *J* = 6.3 Hz), 2.35 (t, 4H, *J* = 7.4 Hz), 2.32 (t, 4H, *J* = 6.9 Hz), 2.07 (t, 8H, *J* = 6.9 Hz), 2.05 (t, 8H, *J* = 6.9 Hz), 1.61 (m, 9H), 1.42-1.25 (m, 56H), 0.91 (m, 12H); ^{13}C NMR (100 MHz, CD_3OD:$CDCl_3$ = 1:1): δ 174.88 (2C), 174.54 (2C), 130.93 (4C), 130.83 (4C), 129.05 (4C), 128.96 (4C), 71.77, 71.66, 71.20, 67.55, 67.26, 64.65 (2C), 63.70 (2C), 35.13 (2C), 34.97 (2C), 32.57 (4C), 30.68 (4C), 30.39 (8C), 30.32 (2C), 30.28 (2C), 30.22 (2C), 30.19, 30.15, 28.15 (8C), 26.56 (4C), 25.95 (2C), 25.92 (2C), 23.56 (4C), 14.58 (4C); ESI-MS (m/z): 723.9 $[M-2NH_4]^{2-}$, 1448.0 $[M-2NH_3-H]^-$.

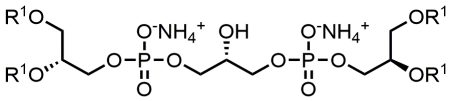

CL(16:0-16:0/16:0-16:0) (R^1: palmitoyl)

CL(16:0-16:0/16:0-16:0) was synthesized according to the previous method (Scheme 1, refs. 1 and 2), except that palmitic acid was used in place of oleic acid: ^{1}H NMR (400 MHz, $CDCl_3$): δ 5.23 (m, 2H), 4.47 (dd, 2H, *J* = 12.0, 3.2 Hz), 4.19 (dd, 2H, *J* = 12.0, 6.7 Hz), 4.01 (d, 2H, *J* = 5.6 Hz), 4.00 (d, 2H, *J* = 5.6 Hz), 3.95-3.87 (m, 5H), 2.34 (t, 4H, *J* = 7.2 Hz), 2.31 (t, 4H, *J* = 7.6 Hz), 1.60 (m, 9H), 1.38-1.21 (m, 96H), 0.90 (t, 12H, *J* = 6.8 Hz); ^{13}C NMR (125 MHz, $CDCl_3$): δ 174.16 (4C), 70.58 (2C), 70.51, 66.33 (2C), 63.39 (2C), 62.35 (2C), 33.76 (2C), 33.58 (2C), 31.68(4C), 29.43 (4C), 29.38 (4C), 29.32 (8C), 29.29 (4C), 29.15 (4C), 29.09 (4C), 28.87 (4C), 28.85 (4C), 24.67 (4C), 24.64 (4C), 22.33 (4C), 13.03 (4C); ESI-MS (m/z): 675.9 $[M-2NH_4]^{2-}$, 1352.1 $[M-2NH_3-H]^-$.

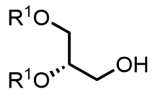

1 (R: oleoyl)

1 was synthesized according to the previous method (Scheme 1, ref. 2): ^{1}H NMR (500 MHz, $CDCl_3$): δ 5.34 (m, 4H), 5.18 (tt, 1H, *J* = 10.0, 5.0 Hz), 4.31 (dd, 1H, *J* = 11.9, 4.5 Hz), 4.23 (dd, 1H, *J* = 11.9, 5.6 Hz), 3.71 (dd, 2H, *J* = 5.4, 1.6 Hz), 2.34 (t, 2H, *J* = 7.5 Hz), 2.32 (t, 2H, *J* = 7.7 Hz), 2.00 (m, 8H), 1.61 (m, 5H), 1.38-1.17 (m, 40H), 0.88 (m, 6H); ^{13}C NMR (100 MHz, $CDCl_3$): δ 173.70, 173.36, 130.03 (2C), 129.69 (2C), 72.14, 62.00, 61.59, 34.27, 34.09, 31.90 (2C), 29.76 (2C), 29.70 (2C), 29.52 (2C), 29.44, 29.32 (2C), 29.30 (2C), 29.16 (2C), 29.10 (2C), 29.06, 27.22 (2C), 27.16 (2C), 24.92, 24.87, 22.67 (2C), 14.08 (2C); ESI-MS (m/z): 643.5 $[M+Na]^+$.

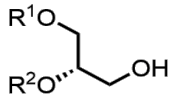

2 (R^1: linoleoyl, R^2: oleoyl)

2 was synthesized according to the previous method (Scheme 2, refs. 1 and 3), except that oleic acid was used in place of stearic acid, in a 16% yield for 4 steps as a colorless oil: ^{1}H NMR (400 MHz, $CDCl_3$): δ 5.33 (m, 6H), 5.08 (tt, 1H, *J* = 10.0, 5.8 Hz), 4.32 (dd, 1H, *J* = 11.9, 4.6 Hz), 4.23 (dd, 1H, *J* = 11.9, 5.6 Hz), 3.73 (m, 2H), 2.77 (m, 2H), 2.34 (t, 2H, *J* = 7.6 Hz), 2.32 (t, 2H, *J* = 7.9 Hz), 2.03 (m, 8H), 1.60 (m, 5H), 1.39-1.21 (m, 34H), 0.88 (m, 6H); ^{13}C NMR (100 MHz, $CDCl_3$): δ 173.95, 173.60, 130.44, 130.24, 130.21, 129.90, 128.29, 128.10, 72.32, 62.21, 61.77, 34.48, 34.29, 32.12, 31.74, 29.98, 29.91, 29.82, 29.73, 29.56 (2C), 29.53 (2C), 29.38 (2C), 29.32 (2C), 29.27, 27.43, 27.41, 27.40, 27.38, 25.84, 25.13, 25.08, 22.89, 22.78, 14.32, 14.28; ESI-MS (m/z): 619.6 $[M+H]^+$, 641.6 $[M+Na]^+$.

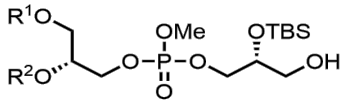

3 (R^1: linoleoyl, R^2: oleoyl)

3 was synthesized according to the previous method (Scheme 2, refs. 1 and 3), except that **2** was used as a starting material, in a 28% yield for 4 steps as a colorless oil: ^{1}H NMR (400 MHz, $CDCl_3$): δ 5.33 (m, 6H), 5.22 (m, 1H), 4.33 (dd, 1H, *J* = 12.0, 4.0 Hz), 4.19 (m, 3H), 4.05 (m, 2H), 3.92 (m, 1H), 3.78 (dd, 3H, *J* = 11.2, 5.2 Hz), 3.63 (m, 2H), 2.77 (t, 2H, *J* = 7.0 Hz), 2.34 (t, 2H, *J* = 7.5 Hz), 2.31 (t, 2H, *J* = 9.2 Hz), 2.04 (m, 8H), 1.62 (m, 5H), 1.40-1.22 (m, 34H), 0.90 (m, 15H), 0.10 (s, 6H); ^{13}C NMR (100 MHz, $CDCl_3$): δ 173.44, 173.00, 130.44, 130.23, 130.20, 129.91, 128.29, 128.10, 71.30, 69.62, 67.90, 65.79, 63.22, 61.82, 54.80, 34.34, 34.21, 32.11, 31.73, 29.98, 29.92, 29.83, 29.73, 29.55, 29.53, 29.41 (2C), 29.34 (3C), 29.31, 29.27, 27.41 (4C), 25.93 (3C), 25.84, 25.02 (2C), 22.89, 22.78, 18.26, 14.32, 14.28, -4.51, -4.64; ESI-MS (m/z): 918.8 $[M+H_3O]^+$, 939.7 $[M+K]^+$.

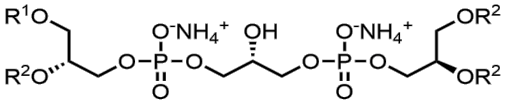

CL(18:2-18:1/18:1-18:1) (R^1: linoleoyl, R^2: oleoyl)

CL(18:2-18:1/18-1-18:1) was synthesized according to the previous method (Scheme 1, refs. 1 and 3), except that phosphoramidation was carried out using **3** and **1**, in a 18% yield for 5 steps as a colorless oil: ^{1}H NMR (500 MHz, CD_3OD:$CDCl_3$ = 1:1): δ 5.34 (m, 10H), 5.24 (m, 2H), 4.42 (dd, 2H, *J* = 12.0, 2.6 Hz), 4.19 (dd, 2H, *J* = 12.0, 6.8 Hz), 4.03-3.90 (m, 9H), 2.78 (t, 2H, *J* = 6.6 Hz), 2.34 (t, 4H, *J* = 8.1 Hz), 2.33 (t, 4H, *J* = 8.0 Hz), 2.04 (m, 16H), 1.62 (m, 9H), 1.39-1.25 (m, 74H), 0.90 (m, 12H); ^{13}C NMR (125 MHz, CD_3OD:$CDCl_3$ = 1:1): δ 174.55 (2C), 174.19 (2C), 130.73 (2C), 130.58, 130.55, 130.31 (2C), 128.70 (2C), 128.55 (2C), 71.17 (2C), 70.52, 66.69 (2C), 64.40 (2C), 63.28 (2C), 34.83 (2C), 34.68 (2C), 32.53 (3C), 32.15, 30.37 (6C), 30.31 (2C), 30.26 (2C), 30.12 (3C), 29.96 (2C), 29.92 (4C), 29.88 (3C), 29.84 (2C), 29.75 (3C), 29.73 (2C), 27.80 (8C), 26.23, 25.53 (2C),25.49 (2C), 23.25 (3C), 23.15, 14.42 (2C), 14.40 (2C); ESI-MS (m/z): 726.8 $[M-2NH_4]^{2-}$, 1454.0 $[M-2NH_3-H]^-$.

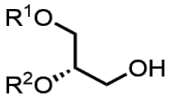

4 (R^1: oleoyl, R^2: linoleoyl)

4 was synthesized by the similar method to that used for the synthesis of **2** (Scheme 2, refs. 1 and 3), except that OH group of the *sn*-2 position was esterified by linoleic acid after esterification of OH group of the *sn*-1 position by oleic acid, in a 43% yield for 4 steps as a colorless oil: ^{1}H NMR (400 MHz, $CDCl_3$): δ 5.33 (m, 6H), 5.08 (tt, 1H, *J* = 10.0, 5.1 Hz), 4.32 (dd, 1H, *J* = 11.9, 4.6 Hz), 4.23 (dd, 1H, *J* = 11.9, 5.6 Hz), 3.73 (m, 2H), 2.77 (m, 2H), 2.35 (t, 2H, *J* = 7.4 Hz), 2.32 (t, 2H, *J* = 7.7 Hz), 2.04 (m, 8H), 1.62 (m, 5H), 1.39-1.21 (m, 34H), 0.88 (m, 6H); ^{13}C NMR (100 MHz, $CDCl_3$): δ 173.95, 173.58, 130.44, 130.24, 130.20, 129.91, 128.30, 128.10, 72.33, 62.20, 61.77, 34.48, 34.30, 32.12, 31.74, 29.98, 29.91, 29.82, 29.73, 29.56 (2C), 29.53 (2C), 29.38 (2C), 29.32 (2C), 29.27, 27.43, 27.41, 27.40, 27.38, 25.84, 25.13, 25.08, 22.89, 22.78, 14.41,14.32; ESI-MS (m/z): 619.6 $[M+H]^+$, 641.6 $[M+Na]^+$.

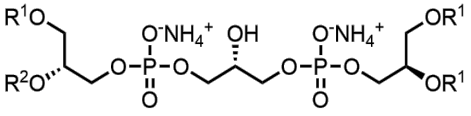

CL(18:1-18:2/18:1-18:1) (R^1: oleoyl, R^2: linoleoyl)

CL(18:1-18:2/18:1-18:1) was synthesized according to the procedure similar to that used for the synthesis of CL(18:2-18:1/18:1-18:1) (Scheme 2, refs. 1 and 3), except that **4** was used as a starting material, in a 42% yield for 8 steps as a colorless oil: ^{1}H NMR (500 MHz, CD_3OD:$CDCl_3$ = 1:1): δ 5.35 (m, 10H), 5.24 (tt, 2H, *J* = 8.5, 5.5 Hz), 4.44 (dd, 2H, *J* = 12.0, 3.2 Hz), 4.20 (dd, 2H, *J* = 12.0, 6.8 Hz), 4.00 (t, 4H, *J* = 5.8 Hz), 3.93 (m, 5H), 2.78 (t, 2H, *J* = 6.6 Hz), 2.35 (t, 4H, *J* = 7.6 Hz), 2.33 (t, 4H, *J* = 7.7 Hz), 2.05 (m, 16H), 1.61 (m, 9H), 1.40-1.23 (m, 74H), 0.90 (m, 12H); ^{13}C NMR (125 MHz, CD_3OD:$CDCl_3$ = 1:1): δ 174.68 (2C), 174.03 (2C), 130.78 (2C), 130.65, 130.63, 130.42 (2C), 128.79 (2C), 128.67 (2C), 71.36, 71.30, 70.84, 67.10, 67.05, 64.36, 64.32, 63.40

(2C), 34.92 (2C), 34.77 (2C), 32.64 (3C), 32.26, 30.48 (6C), 30.39 (4C), 30.23 (3C), 30.07 (2C), 30.03 (4C), 30.00 (3C), 29.95 (2C), 29.86 (3C), 29.83 (2C), 27.89 (8C), 26.32, 25.64 (2C),25.62 (2C), 23.36 (3C), 23.26, 14.47 (4C); ESI-MS (m/z): 726.8 $[M-2NH_4]^{2-}$, 1454.1 $[M-2NH_3-H]^-$.

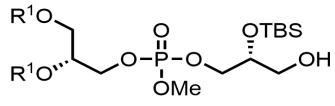

5 (R^1: linoleoyl)

5 was synthesized according to the previous method (Scheme 1, refs. 1 and 2), except that linoleic acid was used in place of stearic acid, in a 9% yield for 11 steps as a colorless oil: ^{1}H NMR (400 MHz, $CDCl_3$): δ 5.38 (m, 8H), 5.23 (m, 1H), 4.33 (dd, 1H, *J* = 12.0, 4.4 Hz), 4.24-4.10 (m, 3H), 4.04 (m, 2H), 3.92 (m, 1H), 3.77 (dd, 3H, *J* = 11.2, 5.2 Hz), 3.63 (m, 2H), 2.76 (t, 4H, *J* = 6.8 Hz), 2.33 (t, 2H, *J* = 7.6 Hz), 2.30 (t, 2H, *J* = 7.8 Hz), 2.05 (t, 4H, *J* = 6.8 Hz), 2.03 (t, 4H, *J* = 6.8 Hz), 1.61 (m, 5H), 1.40-1.20 (m, 28H), 0.88 (m, 15H), 0.10 (s, 6H); ^{13}C NMR (100 MHz, $CDCl_3$): δ 173.42, 173.00, 130.44 (2C), 130.21 (2C), 128.29 (2C), 128.10 (2C), 71.37, 69.54, 67.88, 65.78, 63.23, 61.82, 54.80, 34.33, 34.20, 31.74 (2C), 29.83 (2C), 29.55 (2C), 29.41 (2C), 29.34 (2C), 29.30, 29.27, 27.41 (4C), 25.93 (3C), 25.84 (2C), 25.02 (2C), 22.78 (2C), 18.26, 14.28 (2C), -4.51,-4.64; ESI-MS (m/z): 899.7 $[M+H]^+$, 921.7 $[M+Na]^+$, 937.7 $[M+K]^+$.

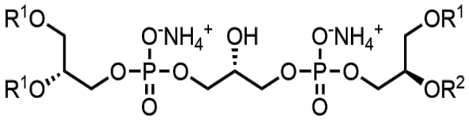

CL(18:2-18:2/18:2-18:1) (R^1: linoleoyl, R^2: oleoyl)

CL(18:2-18:2/18:2-18:1) was synthesized according to the previous method (Scheme 1, refs. 1 and 3), except that phosphoramidation was carried out using **5** and **2**, in a 16% yield for 9 steps as a colorless oil: ^{1}H NMR (500 MHz, CD_3OD:$CDCl_3$ = 1:1): δ 5.32 (m, 14H), 5.24 (m, 2H), 4.45 (dd, 2H, *J* = 12.0, 3.1 Hz), 4.20 (dd, 2H, *J* = 12.0, 6.8 Hz), 4.00 (t, 4H, *J* = 5.7 Hz), 3.93 (m, 5H), 2.78 (t, 6H, *J* = 6.6 Hz), 2.35 (t, 4H, *J* = 7.5 Hz), 2.33 (t, 4H, *J* = 7.5 Hz), 2.05 (m, 16H), 1.61 (m, 9H), 1.40-1.27 (m, 62H), 0.90 (m, 12H); ^{13}C NMR (125 MHz, CD_3OD:$CDCl_3$ = 1:1): δ 174.86 (2C), 174.51 (2C), 130.89 (2C), 130.76 (2C), 130.58 (2C), 128.94 (4C), 128.84 (4C), 71.62, 71.52, 71.09, 67.32, 67.27, 64.53, 64.49, 63.62 (2C), 35.06 (2C), 34.90 (2C), 32.80, 32.42 (3C), 30.66 (2C), 30.54 (2C), 30.52 (2C), 30.38 (2C), 30.23 (4C), 30.18 (2C), 30.15 (2C), 30.11 (2C), 30.06 (2C), 30.03 (2C), 30.01, 28.03 (8C), 26.46 (3C), 25.81 (2C), 25.78 (2C), 23.51, 23.40 (3C), 14.51 (4C); ESI-MS (m/z): 724.8 $[M-2NH_4]^{2-}$, 1450.1 $[M-2NH_3-H]^-$.

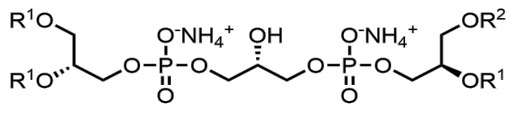

CL(18:2-18:2/18:1-18:2) (R^1: linoleoyl, R^2: oleoyl)

CL(18:2-18:2/18:1-18:2) was synthesized according to the previous method (Scheme 1, refs. 1 and 3), except that phosphoramidation was carried out using **5** and **4**, in a 17% yield for 9 steps as a colorless oil: ^{1}H NMR (400 MHz,

CD_3OD:$CDCl_3$ = 1:1): δ 5.33 (m, 14H), 5.24 (m, 2H), 4.45 (dd, 2H, *J* = 12.0, 3.1 Hz), 4.21 (dd, 2H, *J* = 12.0, 6.7 Hz), 4.00 (t, 4H, *J* = 5.6), 3.93 (m, 5H), 2.77 (t, 6H, *J* = 6.3), 2.35 (t, 4H, *J* = 7.4 Hz), 2.33 (t, 4H, *J* = 7.6 Hz), 2.05 (m, 16H), 1.62 (m, 9H), 1.42-1.25 (m, 62H), 0.90 (m, 12H); ^{13}C NMR (125 MHz, CD_3OD:$CDCl_3$ = 1:1): δ 174.84 (2C), 174.92 (2C), 130.89 (2C), 130.77 (2C), 130.60 (2C), 128.96 (4C), 128.86 (4C), 71.65, 71.59, 67.34 (2C), 64.51 (2C), 63.62 (2C), 35.07 (2C), 34.92 (2C), 32.83, 32.45 (3C), 30.65 (2C), 30.57 (2C), 30.55 (2C), 30.41 (2C), 30.26 (4C), 30.22 (2C), 30.18 (2C), 30.14 (2C), 30.09 (2C), 30.04 (3C), 28.08 (2C), 28.05 (6C), 26.48 (4C), 25.84 (2C), 25.80 (2C), 23.53, 23.43 (3C), 14.52 (4C); ESI-MS (m/z): 724.8 $[M-2NH_4]^{2-}$, 1450.1 $[M-2NH_3-H]^-$.

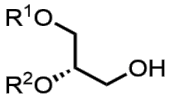

6 (R^1: oleoyl, R^2: palmitoyl)

6 was synthesized according to the procedure similar to that used for the synthesis of **2** (Scheme 2, refs. 1 and 3), except that OH group of the *sn*-2 position was esterified by palmitic acid after esterification of OH group of the *sn*-1 position by oleic acid, in a 43% yield for 4 steps as a colorless oil: ^{1}H NMR (400 MHz, $CDCl_3$): δ 5.33 (m, 4H), 5.08 (tt, 1H, *J* = 4.9, 4.9 Hz), 4.32 (dd, 1H, *J* = 11.9, 4.6 Hz), 4.23 (dd, 1H, *J* = 11.9, 5.6 Hz), 3.72 (m, 2H), 2.34 (t, 2H, *J* = 7.6 Hz), 2.32 (t, 2H, *J* = 7.6 Hz), 2.01 (m, 4H), 1.61 (m, 5H), 1.39-1.21 (m, 48H), 0.87 (t, 6H, *J* = 6.8 Hz); ^{13}C NMR (125 MHz, $CDCl_3$): δ 173.72, 173.41, 130.30, 129.70, 72.14, 61.99, 61.61, 34.30, 31.92, 31.90, 29.76, 29.69 (4C), 29.65 (3C), 29.61, 29.52, 29.47, 29.35, 29.32, 29.30, 29.26, 29.16, 29.09 (2C), 27.22, 27.17, 24.95, 24.88, 22.67 (2C), 14.09 (2C); ESI-MS (m/z): 595.5 $[M+H]^+$, 617.4 $[M+Na]^+$.

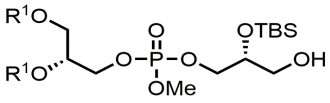

7 (R^1: oleoyl)

7 was synthesized according to the previous method (Scheme 1, refs. 1 and 3), except that oleic acid was used in place of stearic acid, in a 11% yield for 11 steps as a colorless oil: ^{1}H NMR (400 MHz, $CDCl_3$): δ 5.34 (m, 4H), 5.22 (m, 1H), 4.33 (dd, 1H, *J* = 4.4, 11.9 Hz), 4.17 (m, 3H), 4.04 (m, 2H), 3.42 (m, 1H), 3.78 (dd, 3H, *J* = 11.2, 5.2 Hz), 3.63 (dd, 1H, *J* = 8.0, 4.6 Hz), 3.60 (dd, 1H, *J* = 8.0, 4.2 Hz), 2.36 (t, 2H, *J* = 7.6 Hz), 2.33 (t, 2H, *J* = 7.8 Hz), 2.00 (m, 8H), 1.60 (m, 5H), 1.38-1.19 (m, 40H), 0.88 (m, 15H), 0.10 (s, 6H); ^{13}C NMR (100 MHz, $CDCl_3$): δ 173.44, 173.01, 130.23 (2C), 129.91 (2C), 71.38, 69.54, 67.94, 65.78, 63.24, 61.82, 54.81, 34.13, 34.00, 31.12 (2C), 29.98 (2C), 29.93 (2C), 29.87, 29.74 (2C), 29.53 (2C), 29.41 (2C), 29.34 (2C), 29.31, 29.28, 29.19, 27.44 (2C), 27.39 (2C), 25.93 (3C), 25.03 (2C), 22.89 (2C), 18.26, 14.32 (2C), -4.51, -4.64; ESI-MS (m/z): 903.9 $[M+H]^+$.

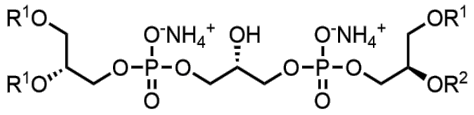

CL(18:1-18:1/18:1-16:0) (R^1: oleoyl, R^2: palmitoyl)

CL(18:1-18:1/18:1-16:0) was synthesized according to the previous method (Scheme 2, refs. 1 and 3), except that phosphoramidation was carried out using **7** and **6**, in a 16% yield for 9 steps as a colorless oil: ^{1}H NMR (500 MHz, CD_3OD:$CDCl_3$ = 1:1): δ 5.32 (m, 6H), 5.24 (tt, 2H, *J* = 9.4, 5.3 Hz), 4.45 (dd, 2H, *J* = 12.1, 3.2 Hz), 4.20 (dd, 2H, *J* = 11.6, 6.5 Hz), 4.00 (t, 4H, *J* = 5.6 Hz), 3.92 (m, 5H), 2.34 (t, 4H, *J* = 7.5 Hz), 2.32 (t, 4H, *J* = 7.5 Hz), 2.03 (m, 12H), 1.61 (m, 9H), 1.48-1.20 (m, 84H), 0.90 (t, 12H, *J* = 6.1 Hz); ^{13}C NMR (125 MHz, CD_3OD:$CDCl_3$ = 1:1): δ 174.83 (2C), 174.52, 130.81 (2C), 130.64 (4C), 71.70 (2C), 71.64 , 67.43 (2C), 64.61 (2C), 63.64 (2C), 35.12 (2C), 34.94 (2C), 32.89 (4C), 30.70 (4C), 30.66 (8C), 30.61 (2C), 30.52(2C), 30.46 (2C), 30.34 (2C), 30.31 (2C), 30.27 (2C), 30.23 (2C), 30.20 (2C), 30.10 (4C), 28.09 (9C), 25.91 (2C), 25.86 (2C), 23.58 (4C), 14.54 (4C); ESI-MS (m/z): 714.7 $[M-2NH_4]^{2-}$, 1429.9 $[M-2NH_3-H]^-$.

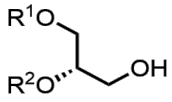

8 (R^1: palmitoyl, R^2: oleoyl)

8 was synthesized by the procedure similar to that used for the synthesis of **2** (Scheme 2, refs. 1 and 3), except that palmitic acid was used in place of linoleic acid, in a 52% yield for 4 steps as a colorless oil: ^{1}H NMR (400 MHz, $CDCl_3$): δ 5.34 (m, 2H), 5.08 (tt, 1H, *J* = 5.2, 4.9 Hz), 4.32 (dd, 1H, *J* = 11.9, 4.5 Hz), 4.23 (dd, 1H, *J* = 11.9, 5.6 Hz), 3.73 (s, 2H), 2.35 (t, 2H, *J* = 7.5 Hz), 2.32 (t, 2H, *J* = 7.7 Hz), 2.08 (br s, 1H), 2.02 (m, 4H), 1.61 (m, 4H), 1.35-1.25 (m, 44H), 0.88 (t, 6H, *J* = 6.8 Hz); ^{13}C NMR (100 MHz, $CDCl_3$): δ 173.80, 173.44, 130.04, 129.70, 72.13, 62.00, 61.57, 34.28, 34.12, 31.93 (2C), 29.77, 29.67 (4C), 29.66 (3C), 29.62, 29.53, 29.48, 29.36, 29.33 (2C), 29.27, 29.18, 29.13 (2C), 29.07, 27.23, 27.17, 24.93, 24.90, 22.69, 14.11 (2C); ESI-MS (m/z): 595.6 $[M+H]^+$, 612.6 $[M+H_3O]^+$.

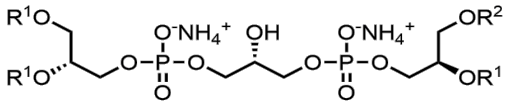

CL(18:1-18:1/16:0-18:1) (R^1: oleoyl, R^2: palmitoyl)

CL(18:1-18:1/16:0-18:1) was synthesized according to the previous method (Scheme 2, refs. 1 and 3), except that phosphoramidation was carried out using **7** and **8**, in a 15% yield for 9 steps as a colorless oil: ^{1}H NMR (400 MHz, CD_3OD:$CDCl_3$ = 1:1): δ 5.32 (m, 6H), 5.24 (m, 2H), 4.43 (dd, 2H, *J* = 12.0, 3.0 Hz), 4.19 (dd, 2H, *J* = 11.0, 6.8 Hz), 4.00 (m, 4H), 3.92 (m, 5H), 2.34 (t, 4H, *J* = 7.7 Hz), 2.33 (t, 4H, *J* = 7.8 Hz), 2.03 (m, 12H), 1.61 (m, 8H), 1.38-1.23 (m, 84H), 0.89 (t, 12H, *J* = 6.0 Hz); ^{13}C NMR (100 MHz, CD_3OD:$CDCl_3$ = 1:1): δ 173.89, 173.85, 173.47 (2C), 129.82 (3C), 129.55 (3C), 70.43, 70.34, 66.14, 66.09, 63.49, 63.44, 62.52 (3C), 34.07 (2C), 33.94 (2C), 31.79 (4C), 29.62 (6C), 29.57 (7C), 29.53 (3C), 29.39 (3C), 29.23 (2C), 29.19 (5C), 29.16 (3C), 29.11, 29.04 (6C), 28.98 (2C), 27.04 (4C), 24.78 (2C), 22.52 (4C), 13.69 (4C); ESI-MS (m/z): 714.7 $[M-2NH_4]^{2-}$, 1429.9

$[M-2NH_3-H]^-$.

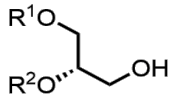

9 (R^1: oleoyl, R^2: palmitoleoyl)

9 was synthesized by the procedure similar to that used for the synthesis of **2** (Scheme 2, refs. 1 and 3), except that OH group of the *sn*-2 position was esterified by palmitoleoic acid after esterification of OH group of the *sn*-1 position by oleic acid, in a 43% yield for 4 steps as a colorless oil: ^{1}H NMR (500 MHz, $CDCl_3$): δ 5.34 (m, 4H), 5.08 (tt, 1H, *J* = 10.1, 5.1 Hz), 4.32 (dd, 1H, *J* = 12.0, 4.6 Hz), 4.24 (dd, 1H, *J* = 12.0, 5.6 Hz), 3.73 (m, 2H), 2.35 (t, 2H, *J* = 7.5 Hz), 2.32 (t, 2H, *J* = 8.2 Hz), 2.01 (m, 8H), 1.62 (m, 5H), 1.47-1.21 (m, 36H), 0.88 (m, 6H); ^{13}C NMR (125 MHz, $CDCl_3$): δ 173.59 (2C), 130.26 (2C), 129.93 (2C), 72.38, 62.22, 61.84, 34.51, 34.32, 32.13, 32.01, 30.00, 29.96, 29.93 (2C), 29.75, 29.55, 29.53, 29.39 (2C), 29.33 (3C), 29.29, 29.21, 27.46 (2C), 27.40 (2C), 25.16, 25.11, 22.90, 22.87, 14.31 (2C); ESI-MS (m/z): 610.7 $[M+H_3O]^+$, 615.7 $[M+Na]^+$, 631.7 $[M+K]^+$.

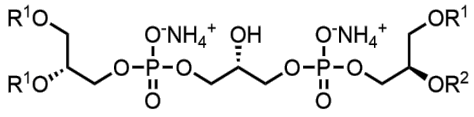

CL(18:1-18:1/18:1-16:1) (R^1: oleoyl, R^2: palmitoleoyl)

CL(18:1-18:1/18:1-16:1) was synthesized according to the previous method (Scheme 2, refs. 1 and 3), except that phosphoramidation was carried out using **7** and **6**, in a 16% yield for 9 steps as a colorless oil: ^{1}H NMR (500 MHz, CD_3OD:$CDCl_3$ = 1:1): δ 5.33 (m, 8H), 5.22 (m, 2H), 4.38 (dd, 2H, *J* = 12.0, 2.9 Hz), 4.17 (dd, 2H, *J* = 11.8, 6.7 Hz), 4.00-3.86 (m, 9H), 2.32 (t, 4H, *J* = 8.5 Hz), 2.31 (t, 4H, *J* = 8.2 Hz), 2.01 (m, 16H), 1.60 (m, 9H), 1.38-1.19 (m, 76H), 0.88 (m, 12H); ^{13}C NMR (125 MHz, CD_3OD: $CDCl_3$ = 1: 1, v/v): δ 173.92 (2C), 173.56 (2C), 130.10 (4C), 129.77 (4C), 70.49, 70.42, 66.23 (2C), 63.72 (2C), 62.68 (3C), 34.30 (2C), 34.15 (2C), 31.97 (2C), 31.85 (2C), 29.81 (8C), 29.59 (4C), 29.38 (8C), 29.30 (2C), 29.23 (6C), 29.18, 29.04, 27.29 (6C), 27.26 (2C), 24.96 (2C), 24.92 (2C), 22.73 (4C), 14.07 (4C); ESI-MS (m/z): 713.8 $[M-2NH_4]^{2-}$, 1428.0 $[M-2NH_3-H]^-$.

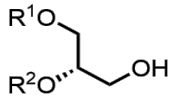

10 (R^1: palmitoleoyl, R^2: oleoyl)

10 was synthesized by the procedure similar to that used for the synthesis of **4** (Scheme 2, refs. 1 and 3), except that palmitoleoic acid was used in place of linoleic acid, in a 52% yield for 4 steps as a colorless oil: ^{1}H NMR (500 MHz, $CDCl_3$): δ 5.34 (m, 4H), 5.08 (tt, 1H, *J* = 10.0, 5.0 Hz), 4.32 (dd, 1H, *J* = 11.9, 4.6 Hz), 4.24 (dd, 1H, *J* = 11.9, 5.7 Hz), 3.73 (m, 2H), 2.35 (t, 2H, *J* = 7.5 Hz), 2.32 (t, 2H, *J* = 7.7 Hz), 2.02 (m, 8H), 1.62 (m, 5H), 1.39-1.20 (m, 36H), 0.88 (m, 6H); ^{13}C NMR (125 MHz, $CDCl_3$): δ 173.93, 173.59, 130.26 (2C), 129.94 (2C), 72.38, 62.23, 61.83, 34.51, 34.32, 32.13, 32.01, 30.00, 29.96, 29.92 (2C), 29.75, 29.55 (2C), 29.39 (2C), 29.32 (3C), 29.29, 29.21, 27.46 (2C), 27.39 (2C), 25.16, 25.11, 22.90, 22.87, 14.30 (2C); ESI-MS (m/z): 610.6

$[M+H_3O]^+$, 615.6 $[M+Na]^+$, 615.6 $[M+K]^+$.

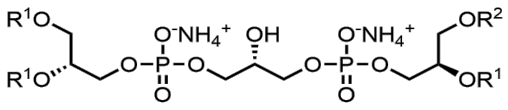

CL(18:1-18:1/16:1-18:1) (R^1: oleoyl, R^2: palmitoleoyl)

CL(18:1-18:1/16:0-18:1) was synthesized according to the previous method (Scheme 2, refs. 1 and 3), except that phosphoramidation was carried out using **7** and **8**, in a 15% yield for 9 steps as a colorless oil: ^{1}H NMR (500 MHz, CD_3OD:$CDCl_3$ = 1:1): δ 5.34 (m, 8H), 5.23 (tt, 2H, *J* = 8.7, 5.5 Hz), 4.42 (dd, 2H, *J* = 12.1, 3.0 Hz), 4.1 (dd, 2H, *J* = 12.0, 6.8 Hz), 3.98 (m, 4H), 3.91 (m, 5H), 2.34 (t, 4H, *J* = 8.4 Hz), 2.32 (t, 4H, *J* = 8.1 Hz), 2.02 (m, 16H), 1.61 (m, 9H), 1.39-1.22 (m, 76H), 0.89 (m, 12H); ^{13}C NMR (125 MHz, CD_3OD:$CDCl_3$ = 1:1): δ 174.46 (2C), 174.08 (2C), 130.48 (4C), 130.20 (4C), 71.03, 70.97, 69.09 (2C), 66.69 (2C), 63.15 (3C), 34.72 (2C), 34.57 (2C), 32.39 (2C), 32.28 (2C), 30.24 (5C), 30.21 (4C), 30.00 (4C), 29.79 (8C), 29.74, 29.70, 29.62 (6C), 29.45, 27.69 (8C), 25.40 (2C), 25.36 (2C), 23.13 (4C), 14.36 (4C); ESI-MS (m/z): 713.7 $[M-2NH_4]^{2-}$, 1427.9 $[M-2NH_4+H]^-$.

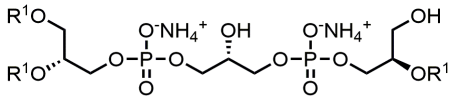

***sn*-1'-MLCL(18:1-18:1/OH-18:1)** (R^1: oleoyl)

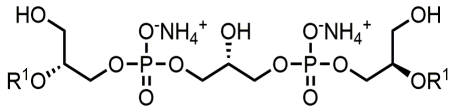

***sn*-1/*sn*-1'-DLCL(OH-18:1/OH-18:1)** (R^1: oleoyl)

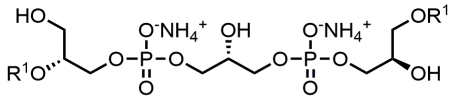

***sn*-1/*sn*-2'-DLCL(OH-18:1/18:1-OH)** (R^1: oleoyl)

A mixture of CL(18:1-18:1/18:1-18:1) (8.0 mg, 5.49 μmol), Triton X-100 (8.0 mg) and *Mucor javanicus* lipase (4.5 mg, 3.7 kU) in 1.0 mL boric acid-borax buffer (50 mM, pH 6.0) was stirred at 37 °C for 4 h. The reaction mixture was quenched by the addition of 5% acetic acid and MeOH. The resulting mixture was filtered and concentrated under reduced pressure. Crude products contained *sn*-1-MLCL(18:1-18:1/OH-18:1) and *sn*-1/*sn*-1'-DLCL(OH-18:1/OH-18:1). *sn*-1/*sn*-2'-DLCL(OH-18:1/18:1-OH) was formed by automigration of *sn*-1/*sn*-1'-DLCL(OH-18:1/OH-18:1). These three derivatives were purified by silica gel column chromatography ($CHCl_3$:MeOH:H_2O = 95:5:0.4 to 70:30:2) and HPLC (Inertsil® Diol column, 2 mL/min, 30°C, $CHCl_3$:MeOH:NH_3OH = 95:5:0.3 to 70:30:1) to give *sn*-1'-MLCL(18:1-18:1/OH-18:1) (0.92 mg, 0.77 μmol, 14%), *sn*-1/*sn*-1'-DLCL(OH-18:1/OH-18:1) (0.51 mg, 0.55 μmol, 10%) and *sn*-1/*sn*-2'-DLCL(OH-18:1/18:1-OH) (0.46 mg, 0.50 μmol, 9%) as a colorless oil: **[*sn*-1'-MLCL(18:1-18:1/OH-18:1)]** ^{1}H NMR (500 MHz, CD_3OD: $CDCl_3$=1:1, v/v): δ 5.34 (m, 6H), 5.23 (m, 1H), 4.97 (m, 1H), 4.40 (m, 1H), 4.15 (m, 1H), 4.10-3.90 (m, 9H), 3.73 (m, 2H), 2.33 (m, 6H), 2.02 (m, 13H), 1.61 (m, 7H), 1.40-1.20 (m, 60H), 0.89 (t, 9H, *J* = 8.2 Hz); ^{13}C NMR (125 MHz, CD_3OD: $CDCl_3$ = 1: 1, v/v): δ 174.75 (2C), 174.16, 130.73 (4C), 130.51 (2C), 71.50 (2C), 71.00, 64.45

(2C), 63.50 (2C), 60.86 (2C), 35.01 (2C), 34.85, 32.74 (3C), 30.57 (6C), 30.46 (2C), 30.32 (3C), 30.13 (3C), 30.08 (3C), 30.05, 29.95 (6C), 27.97 (6C), 25.71 (3C), 23.45 (3C), 14.48 (3C); ESI-MS (m/z): 595.6 $[M-2NH_4]^{2-}$, 1191.9 $[M-2NH_3-H]^-$. **[*sn*-1/*sn*-1'-DLCL(OH-18:1/OH-18:1)]** ^{1}H-NMR (400 MHz, CD_3OD:$CDCl_3$=1:1): δ 5.34 (m, 4H), 4.97 (m, 2H), 4.10-3.90 (m, 9H), 3.74 (m, 4H), 2.34 (t, 4H, *J* = 7.4 Hz), 2.02 (m, 9H), 1.61 (m, 5H), 1.38-1.18 (m, 40H), 0.88 (t, 6H, *J* = 6.5 Hz); ^{13}C NMR (125 MHz, CD_3OD:$CDCl_3$ = 1:1): δ 174.36 (2C), 130.83 (2C), 130.67 (2C), 69.76 (2C), 66.16 (6C), 58.32, 34.94 (2C), 32.90 (2C), 30.71 (2C), 30.69 (2C), 30.64, 30.61, 30.47 (2C), 30.28 (2C), 30.22, 30.19, 30.11 (2C), 30.08 (2C), 28.07 (4C), 25.86 (2C), 23.60 (2C), 14.52 (2C); ESI-MS (m/z): 463.4 $[M-2NH_3-2H]^{2-}$, 927.4 $[M-2NH_3-H]^-$. **[*sn*-1/*sn*-2'-DLCL(OH-18:1/18:1-OH)]** ^{1}H-NMR (400 MHz, CD_3OD:$CDCl_3$=1:1): δ 5.33 (m, 4H), 4.97 (m, 2H), 4.09-3.90 (m, 9H), 3.72 (m, 4H), 2.33 (t, 4H, *J* = 7.4 Hz), 2.02 (m, 9H), 1.60 (m, 5H), 1.39-1.17 (m, 40H), 0.88 (t, 6H, *J* = 6.5 Hz); ^{13}C NMR (125 MHz, CD_3OD:$CDCl_3$ = 1:1): δ 174.35 (2C), 130.83 (2C), 130.66 (2C), 69.77 (2C), 66.16 (6C), 58.33, 34.94 (2C), 32.91 (2C), 30.71 (2C), 30.69 (2C), 30.65, 30.61, 30.48 (2C), 30.28 (2C), 30.22, 30.20, 30.11 (2C), 30.08 (2C), 28.07 (4C), 25.87 (2C), 23.60 (2C), 14.52 (2C); ESI-MS (m/z): 463.4 $[M-2NH_3-2H]^{2-}$, 927.4 $[M-2NH_3-H]^-$.

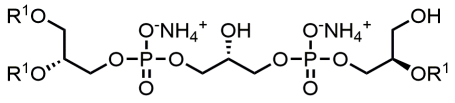

***sn*-1'-MLCL(18:2-18:2/OH-18:2)** (R^1: linoleoyl)

sn-1'-MLCL(18:2-18:2/OH-18:2) was synthesized from CL(18:2-18:2/18:2-18:2) according to the procedure similar to that used for the synthesis of *sn*-1'-MLCL(18:1-18:1/OH-18:1), in a 17 % yield as a colorless oil: ^{1}H NMR (500 MHz, CD_3OD:$CDCl_3$ = 1:1): δ 5.33 (m, 12H), 5.25 (m, 1H), 4.98 (tt, 1H, *J* = 12.4, 6.2 Hz), 4.42 (dd, 1H, *J* = 15.0, 3.6 Hz), 4.17 (dd, 1H, *J* = 15.0, 8.6 Hz), 4.09-3.90 (m, 9H), 3.73 (m, 2H), 2.78 (t, 6H, *J* = 8.4 Hz), 2.34 (m, 6H), 2.07 (t, 6H, *J* = 8.3 Hz), 2.05 (t, 6H, *J* = 8.3 Hz), 1.62 (m, 6H), 1.40-1.24 (m, 44H), 0.89 (m, 9H); ^{13}C NMR (125 MHz, CD_3OD: $CDCl_3$ = 1:1, v/v): δ 174.82 (2C), 174.47, 130.91 (2C), 130.79 (2C), 129.00 (2C), 128.97 (2C), 128.88 (4C), 74.45, 72.77, 71.67, 70.89, 66.85, 64.68, 64.41, 63.63, 61.04, 35.08 (2C), 34.92 (2C), 32.47 (3C), 30.68, 30.57 (2C), 30.28 (6C), 30.19, 30.17, 30.16, 30.10 (2C), 30.07, 28.08 (6C), 26.50 (3C), 25.86, 25.82, 23.45 (3C), 14.51 (3C); ESI-MS (m/z): 592.5 $[M-2NH_4]^{2-}$, 1185.8 $[M-2NH_3-H]^-$.

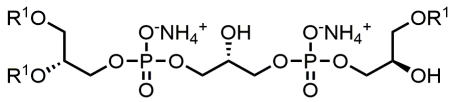

***sn*-2'-MLCL(18:1-18:1/18:1-OH)** (R^1: oleoyl)

A mixture of CL(18:1-18:1/18:1-18:1) (10 mg, 6.87 μmol) and porcine phospholipase A_2 (90 μL, 118 U), 0.50 mM $CaCl_2$ solution (575 μL in distilled water) in 3.0 mL MeOH was stirred at r.t. for 4.5 h. The reaction mixture was filtered and concentrated under reduced pressure. Crude product was purified by silica gel column chromatography ($CHCl_3$:MeOH:H_2O = 95:5:0.4 to 70:30:2) and HPLC (Inertsil® Diol column, 2 mL/min, 30°C, $CHCl_3$:MeOH:NH_3OH = 95:5:0.3 to 70:30:1) to give *sn*-2-MLCL(18:1-18:1/18:1-OH) (1.35 mg, 1.13 μmol, 13%) as a colorless oil: ^{1}H NMR (400 MHz, CD_3OD:$CDCl_3$ = 1:1): δ 5.34 (m, 6H), 5.23 (m, 1H), 4.42 (dd, 1H, *J* = 12.0,

3.0 Hz), 4.18 (dd, 1H, *J* = 12.0, 6.7 Hz), 4.13 (d, 2H, *J* = 5.4 Hz), 4.02-3.73 (m, 10H), 2.35 (t, 2H, *J* = 7.4 Hz), 2.32 (t, 4H, *J* = 7.5 Hz), 2.02 (m, 12H), 1.61 (m, 6H), 1.38-1.18 (m, 62H), 0.89 (t, 9H, *J* = 6.6 Hz); ^{13}C NMR (125 MHz, CD_3OD:$CDCl_3$ = 1:1): δ 175.16, 174.73, 174.40, 130.85, 130.75, 130.73, 130.67, 130.57, 130.49, 71.51, 71.45, 69.57, 67.53, 66.53, 65.92 (2C), 64.55, 63.57, 35.01, 34.85 (2C), 32.74 (3C), 30.56 (6C), 30.38 (2C), 30.32 (3C), 30.13 (3C), 30.10 (3C), 30.05, 29.97 (6C), 27.98 (3C), 27.96 (3C), 25.76, 25.71 (2C), 23.44 (3C), 14.50 (3C); ESI-MS (m/z): 595.5 $[M-2NH_4]^{2-}$, 1191.6 $[M-2NH_3-H]^-$.

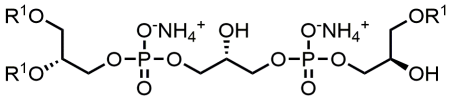

***sn*-2'-MLCL(18:2-18:2/18:2-OH)** (R^1: linoleoyl)

sn-2'-MLCL(18:2-18:2/18:2-OH) was synthesized from CL(18:2-18:2/18:2-18:2) according to the procedure similar to that used for the synthesis of *sn*-2'-MLCL(18:1-18:1/18:1-OH), in a 20 % yield as a colorless oil: ^{1}H-NMR (400 MHz, CD_3OD:$CDCl_3$ = 1:1): δ 5.33 (m, 12H), 5.24 (m, 1H), 4.42 (dd, 1H, *J* = 12.1, 3.0 Hz), 4.18 (dd, 1H, *J* = 12.0, 6.8 Hz), 4.13 (m, 2H), 4.03-3.83 (m, 10H), 2.78 (t, 6H, *J* = 6.8 Hz), 2.36 (t, 2H, *J* = 5.7 Hz), 2.32 (t, 4H, *J* = 7.6 Hz), 2.06 (t, 6H, *J* = 6.7 Hz), 2.04 (t, 6H, *J* = 6.7 Hz), 1.61 (m, 6H), 1.40-1.23 (m, 44H), 0.89 (t, 9H, *J* = 6.8 Hz); ^{13}C-NMR (125 MHz, CD_3OD:$CDCl_3$ = 1:1): δ 175.27, 174.82, 174.47, 130.89 (2C), 130.75 (2C), 128.98 (2C), 128.95 (2C), 128.85 (4C), 71.58, 70.83, 69.75, 67.50, 66.79, 66.06, 64.67, 63.59, 61.39, 35.06, 34.90 (2C), 32.45 (3C), 30.56, 30.54, 30.52, 30.26 (6C), 30.16, 30.12, 30.07 (3C), 30.03, 28.05 (6C), 26.48 (3C), 25.83, 25.79 (2C), 23.43 (3C), 14.50 (3C); ESI-MS (m/z): 592.6 $[M-2NH_4]^{2-}$, 1185.8 $[M-2NH_3-H]^-$.

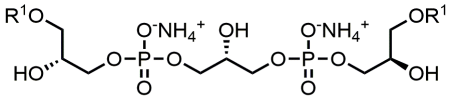

***sn*-2/*sn*-2'-DLCL(18:1-OH/18:1-OH)** (R^1: oleoyl)

sn-2/sn-2'-DLCL(18:1-OH/18:1-OH) was synthesized according to the procedure similar to that used for the synthesis of *sn*-2'-MLCL(18:1-18:1/18:1-OH), except that the reaction time was elongated to 6 h, in a 43 % yield as a colorless oil: ^{1}H NMR (400 MHz, CD_3OD:$CDCl_3$ = 1:1): δ 5.34 (m, 4H), 4.22-4.08 (m, 5H), 4.08-3.96 (m, 6H), 3.96-3-3.87 (m, 4H), 2.36 (t, 4H, *J* = 7.5 Hz), 2.03 (m, 8H), 1.62 (m, 5H), 1.43-1.23 (m, 42H), 0.89 (t, 6H, *J* = 6.5 Hz); ^{13}C NMR (125 MHz, CD_3OD:$CDCl_3$ = 1:1, v/v): δ 174.36 (2C), 130.83 (2C), 130.67 (2C), 69.76 (2C), 66.16 (6C), 58.32, 34.94 (2C), 32.90 (2C), 30.71 (2C), 30.69 (2C), 30.64, 30.61, 30.47 (2C), 30.28 (2C), 30.22, 30.19, 30.11 (2C), 30.08 (2C), 28.07 (4C), 25.86 (2C), 23.60 (2C), 14.52 (2C); ESI-MS (m/z): 463.4 $[M]^{2-}$, 927.4 $[M+H]^-$.

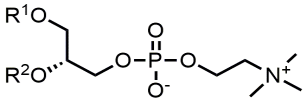

PC(18:1-16:0) (R^1: oleoyl, R^2: palmitoyl)

PC(18:1-16:0) was synthesized according to the previous method (Scheme 2, refs. 1 and 3), except that

phosphoramidation was carried out using **6** and choline tosylate, in a 62% yield for 2 steps as a colorless oil: ^{1}H NMR (500 MHz, $CDCl_3$ = 1:1): δ 5.33 (m, 2H), 5.19 (m, 1H), 4.38 (dd, 2H, *J* = 12.1, 3.0 Hz), 4.28 (m, 2H), 4.11 (dd, 1H, *J* = 12.0, 6.0 Hz), 3.91 (m, 2H), 3.80 (m, 2H), 3.45 (s, 9H), 2.30 (t, 2H, *J* = 7.6 Hz), 2.26 (t, 2H, *J* = 7.6 Hz), 1.56 (m, 4H), 1.35-1.19 (m, 50H), 0.87 (t, 6H, *J* = 6.7 Hz); ^{13}C NMR (125 MHz, $CDCl_3$): δ 173.56, 173.29, 129.98, 129.66, 70.50, 66.24, 63.58, 63.54, 62.98, 59.45, 54.32 (3C), 34.34, 34.13, 31.92, 31.89, 29.74 (5C), 29.67 (2C), 29.63, 29.52, 29.44, 29.36, 29.32 (2C), 29.29 (2C), 29.23, 29.19 (2C), 27.22 (2C), 25.01, 24.89, 22.66 (2C), 14.08 (2C); ESI-MS (m/z): 760.6 $[M+H]^+$.

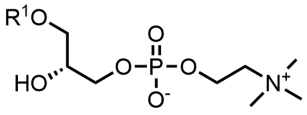

***sn*-2-LPC(18:1-OH)** (R^1: oleoyl)

A mixture of PC(18:1-18:1) (22.9 mg, 29.1 μmol) and porcine phospholipase A_2 (175 μL, 230 U), $CaCl_2$ solution (200 mM in distilled water, 300 μL), Triton X-100 (20 mg) in 3.0 ml Tris-HCl buffer 0.20 M, pH 7.5) was stirred at 37 °C for 23 h. The reaction mixture was quenched with 5% acetic acid and MeOH. The resulting mixture was filtered and concentrated under reduced pressure. The crude product was purified by silica gel column chromatography ($CHCl_3$:MeOH:H_2O = 80:20:2 to 70:30:6) to give *sn*-2-LPC(18:1-OH) (15.0 mg, 28.7 μmol, 99%) as a colorless oil: ^{1}H NMR (400 MHz, CD_3OD:$CDCl_3$ = 1:1): δ 5.34 (m, 2H), 4.37 (m, 2H), 4.09 (m, 2H), 3.99 (m, 2H), 3.84 (m, 3H), 3.77 (m, 1H), 3.36 (s, 9H), 2.32 (t, 2H, *J* = 7.3 Hz), 2.00 (m, 4H), 1.57 (m, 2H), 1.40-1.20 (m, 20H), 0.88 (t, 3H, *J* = 6.7 Hz); ^{13}C NMR (100 MHz, CD_3OD:$CDCl_3$ = 1:1): δ 174.28, 130.20, 129.88, 68.71, 67.52, 66.34, 60.13, 59.38, 54.63 (3C), 32.14 (2C), 30.05, 30.00, 29.77, 29.65, 29.54 (4C), 27.47 (2C), 25.16, 22.90, 14.34; ESI-MS (m/z): 522.4 $[M+H]^+$.

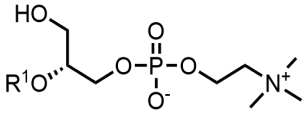

***sn*-1-LPC(OH-18:1)** (R^1: oleoyl)

A mixture of PC(18:1-18:1) (25 mg, 31.8 μmol) and *Mucor javanicus* lipase (25 mg, 21 kU), Triton X-100 (25 mg) in 2.0 ml boric acid-borax buffer (50 mM, pH 6.0) was stirred at 37 °C for 35 min. The reaction mixture was added MeOH, filtered and concentrated under reduced pressure. The crude product was purified by silica gel column chromatography ($CHCl_3$:MeOH:H_2O = 90:10:1 to 70:30:6) to give *sn*-1-LPC(OH-18:1) (16.2 mg, 31.2 μmol, 98%) as a colorless oil: ^{1}H NMR (400 MHz, CD_3OD:$CDCl_3$ = 1:1): δ 5.34 (m, 2H), 4.92 (m, 1H), 4.29 (m, 2H), 4.02 (m, 1H), 3.92 (m, 1H), 3.75 (m, 2H), 3.64 (m, 2H), 3.31 (s, 9H), 2.29 (t, 2H, *J* = 7.4 Hz), 1.99 (m, 5H), 1.57 (m, 2H), 1.40-1.20 (m, 20H), 0.88 (t, 3H, *J* = 6.6 Hz); ^{13}C NMR (100 MHz, CD_3OD:$CDCl_3$ = 1:1): δ 173.68, 130.22, 129.89, 69.23, 66.01, 63.70, 61.35, 60.02, 54.54 (3C), 32.13 (2C), 30.02, 29.99, 29.76, 29.58, 29.54 (2C), 29.47, 29.44, 27.46 (2C), 25.17, 22.90, 14.34; ESI-MS (m/z): 522.4 $[M+H]^-$.

References

1. Abe, M., Kitsuda, S., Ohyama, S., Koubori, S., Murai, M., and Miyoshi, H. (2010) Concise procedure for the synthesis of cardiolipins having different fatty acid combinations, *Tetrahedron Lett*. **51**, 2071-2073.
2. Abe, M., Niibayashi, R., Koubori, S., Moriyama, I., and Miyoshi, H. (2011) Molecular mechanisms for induction of peroxidase activity of cytochrome *c*-cardiolipin complex, *Biochemistry* **50**, 8383-8391.
3. Abe, M., Nakano, M., Kosaka, A., and Miyoshi, H. (2015) Synthesis of photoreactive cardiolipins for a photoaffinity labeling study, *Tetrahedron Lett.* **56**, 2258-2261.

Mechanism for Remodeling of the Acyl Chain Composition of Cardiolipin Catalyzed by *Saccharomyces cerevisiae* Tafazzin

Masato Abe, Yui Hasegawa, Masahide Oku, Yoshiki Sawada, Eriko Tanaka, Yasuyoshi Sakai and Hideto Miyoshi

J. Biol. Chem. published online June 6, 2016